DEVELOPMENT OF
AN INERT CERAMIC ANODE
TO REDUCE ENERGY CONSUMPTION
IN MAGNESIUM PRODUCTION

Final Report

Cooperative Agreement DE-FC07-91 ID13133

THE DOW CHEMICAL COMPANY

DEVELOPMENT OF
AN INERT CERAMIC ANODE
TO REDUCE ENERGY CONSUMPTION
IN MAGNESIUM PRODUCTION

Final Report

Cooperative Agreement DE-FC07-91 ID13133

By

The Dow Chemical Company
1776 Building
Midland, Michigan 48674-1776

Submitted: May 31, 1997

Work Performed Under Cooperative Agreement DE-FC07-91 ID13133

DISCLAIMER

This report was prepared as an account of work sponsored by an agency of the
United States Government. Neither the United States Government nor any
agency thereof, nor any of their employees, makes any warranty, express or
implied, or assumes any legal liability or responsibility for the accuracy,
completeness, or usefulness of any information, apparatus, product, or process
disclosed, or represents that its use would not infringe privately owned rights.
Reference herein to any specific commercial product, process, or service by trade
name, trademark, manufacturer, or otherwise, does not necessarily constitute or
imply its endorsement, recommendation, or favoring by the United States
Government or any agency thereof. The views and opinions of authors expressed
herein do not necessarily state or reflect those of the United States Government or
any agency thereof.

DISCLAIMER

Portions of this document may be illegible
in electronic image products. Images are
produced from the best available original
document.

TABLE OF CONTENTS

TABLE OF CONTENTS (cont.)

LIST OF FIGURES

LIST OF FIGURES (cont.)

LIST OF TABLES

Executive Summary

The objective of this work has been to develop an inert, dimensionally stable anode for the production of magnesium in electrolytic reduction cells presently used by Dow Chemical. This project was partially funded (80%) by the U.S. Department of Energy, Office of Industrial Processes, Conservation and Renewable Technology. A stable anode would allow optimization of the spacing between anode and cathode yielding energy savings of approximately 2 kW-hr per pound of magnesium produced. In addition, the currently used graphite anodes are consumed during electrolysis at a cost of several million dollars every year. There is also considerable projected labor savings from the elimination of the need to reposition the anodes to maintain the anode's electrical efficiency. Not having to adjust the anode would allow better sealing at the furnace/anode interface for substantial environmental benefits. To make laboratory scale anodes, a formulation resulting in a semiconductive ceramic (TiO_2 + Ta^{+5} and TiO_2 + Nb^{+5}) material is formed as a thin walled closed end tube by slip casting and sintering. The tube is then filled with a metal-ceramic composite matched in thermal expansion and serving as the primary current carrier. The anodes are tested in laboratory-scale magnesium cells.

The testing goal for Phase II of the cooperative agreement was to demonstrate six anodes surviving a 30 day test lifetime with acceptable wear rates and electrical performance in a laboratory scale magnesium cell test. In order to accomplish this goal, state of the art slip casting techniques were used and advanced in the pursuit of a virtually flaw free ceramic anode shell. Novel core materials were also invented to allow for the complete, crack free fabrication of the laboratory scale anode. Two successive anodes were tested and exceeded the 30 day cell lifetime goal with excellent wear characteristics. Unfortunately, a notification that the Government portion for Phase III funding would not be available shifted the testing emphasis to more aggressive laboratory tests to evaluate the technical risk associated with continuing the anode replacement project without Government funding. The more aggressive testing revealed that the ceramic anode had a rather narrow operating region. This lack of robustness of the dimensionally stable ceramic anode resulted in the Dow Chemical Company's Magnesium Business making the decision not to continue the project without continued Government support.

Introduction and Background

The objective of this work is to develop a dimensionally stable ceramic anode for production of magnesium metal in electrolytic cells, replacing the graphite anodes currently used by The Dow Chemical Company magnesium business. The implementation of a dimensionally stable anode would have significant financial impact by improving the electrical efficiency of the electrolytic process. Additional savings will also be realized by a reduction in labor costs currently needed to position and feed the graphite anodes which have significant wear rates due to the corrosive nature of the electrolytic process. Not having to adjust the anode would also allow better sealing at the furnace/anode interface for substantial environmental benefits.

Because of the energy savings potential of this work, this project is being partially funded (80%) by the U.S. Department of Energy, Office of Industrial Processes, Conservation and Renewable Technology. The work is based on compositional and design technology for a ceramic anode developed in the former Central Research Inorganic Laboratory[1]. The approach selected is to use a ceramic semiconductor tube as the material to interface with the bath and gaseous atmosphere in the cell. To compensate for the ceramic's higher resistivity compared to graphite, the ceramic is to be prepared as a thin hollow shell (tube) closed at one end. The ceramic shell is then to be filled with a high conductivity, both electrical and thermal, core. The core is to contain a metal component that provides the high conductivity. To compensate for the high thermal expansion of the metal, the core contains ceramic particles in sufficient quantity to minimize the thermally induced stresses between the shell and core. Thus the anode is to be a ceramic tube filled with a metal-ceramic composite core.

This report encompasses the work on developing a dimensionally stable anode during the period of 1/1/91 through 12/31/96.

Economic Analysis

An economic analysis is valuable tool when making any business decision. The following is an economic analysis targeting the potential financial impact of implementing a dimensionally stable ceramic anode into Dow's magnesium processes. The analysis is

reported in the form of change in net present value (NPV), and not in absolute NPV, numbers which have components that are Dow propriety information.

The basis for the model is that the phase III of the Government cooperative agreement would begin in January, 1997 and would concluded successfully in December, 1999. The dimensionally stable anode technology would then be implemented in stages in Dow's production facility and reach full conversion by December, 2004. The model numbers reflect the staged implementation of the replacement anodes at the 10% replacement level of the production anodes in 1999. In 2001, a total of 25% of the production anodes are the new ceramic anodes. Between 2003 and 2005, the remaining graphite anodes are replaced at 25% a year rate. For this analysis, it was assumed that the implementation of the replacement ceramic anodes would not have an effect, neither positive nor negative, on the quality of the magnesium produced or on the production rate. The replacement project would only effect the electrical efficiency and thus the utilities cost, the operating labor, and small fixed capital for implementation. No dollar value is assigned to the positive impact on the environmental issues. The cost for the ceramic anode has been estimated at the cost of the equivalent graphite that is consumed for each anode site over a 2 1/2 year period (the designed lifetime of a ceramic anode). This anode cost estimate has been validated by our scale-up partner. The electrical efficiency of the ceramic anode is assumed to be equivalent to the graphite anodes currently used. The electrical cost used for this analysis was 3.5 cents per kW-hr. The electrical saving achieved by the ceramic anode is based solely on its dimensionally stability. This energy saving is realized in the economic model as a function of the percent of anode implementation. A 10.75% cost of capital was used in the model.

Table I presents the economic value of implementation of a dimensionally stable ceramic anode over a ten year span.

This table reveals that at ten years, the annual net present value (NPV) of the anode replacement project is over $12MM with a cumulative NPV of almost $60MM. The increase in annual profit before taxes is $21MM. The major portion of this savings is the ~$15MM savings from the increased electrical efficiency of the dimensionally stable ceramic anodes.

7

1776 BUILDING
April 30, 1997

Dr. Sara Dillick
U.S. Department of Energy
Office of Industrial Technology
1000 Independence Avenue, SW
Washington, DC 20585-0121

Dear Dr. Dillick:

Enclosed is the Final Technical Report for the Cooperative Agreement
No. DE-FC07-91 ID13133.

Sincerely,

Stephen A. Anderson

Stephen A. Anderson
Ceramics & Advanced Materials
(517) 636-3754

SAA/cjs

Enclosure

DOE F 1332.15
(03-93)
Combines previous
version of DOE
F 1332.15 and .16.
All other editions are
obsolete.

U. S. DEPARTMENT OF ENERGY
RECOMMENDATIONS FOR THE ANNOUNCEMENT AND DISTRIBUTION
OF DEPARTMENT OF ENERGY (DOE) SCIENTIFIC AND TECHNICAL INFORMATION (STI)
(See instructions on reverse side. Use plain bond paper if additional space is needed for explanations.)

OMB Control No.
1910-1400
OMB Burden
Disclosure
Statement on
reverse side

PART I *(DOE, DOE Contractors, Grantees, and Awardees complete)*

A. Product/Report Data

1. (Award) Contract No. DE-FC07-91ID13133

2. Title DEVELOPMENT OF AN INERT CERAMIC ANODE TO REDUCE ENERGY CONSUMPTION IN MAGNESIUM PRODUCTION

3. Product/Report Description

☒ a. Report *(Complete all that apply)*
  (1) ☒ Print ☐ Nonprint *(specify)* _____
  (2) ☐ Quarterly ☐ Semiannual ☐ Annual ☒ Final
    ☐ Topical ☐ Phase I ☐ Phase II
    ☐ Other *(specify)* _____

  Dates covered 12/28/91 thru 12/31/96

☐ b. Conference/Meeting/Presentation *(Complete all that apply)*
  (1) ☐ Print ☐ Nonprint *(specify)* _____
    ☐ Published proceedings
    ☐ Other *(specify)* _____

  (2) Conference Title *(no abbreviations)* _____

  Location *(city/state/country)* _____

  Date(s) *(m/d/y)* __/__/__ thru *(m/d/y)* __/__/__
  Sponsor _____

☐ c. Software—Additional forms are required. Follow instructions on the back of this form.

☐ d. Other *(Provide complete description)* _____

B. Patent Information

Yes No

☐ ☒ Is any new equipment, process, or material disclosed?
    If yes, identify page numbers _____

☐ ☒ Has an invention disclosure been submitted?
    If yes, identify the disclosure number and to whom it was submitted. Disclosure number _____
    Submitted to _____

☐ ☒ Are there patent-related objections to the release of this STI product? If so, state the objections. _____

C. Contact *(Person knowledgeable of content)*

Name STEPHEN A. ANDERSON
Phone (517) 636-3754
Position SR. RESEARCH ENGINEER
Organization THE DOW CHEMICAL COMPANY

PART II *(DOE/DOE Contractors complete/or as instructed by DOE contracting officer)*

A. DOE Identifiers

1. Product/Report Nos. _____

2. Funding Office(s) *(NOTE: Essential data)* _____

B. Copies for Transmittal to AD-21 (OSTI)
(STI must be of sufficient quality for microfilming/copying.)

☐ 1. One for classified processing
☐ 2. _____ *(number)* for standard classified distribution
☐ 3. Two unclassified for processing
☐ 4. _____ *(number)* for program unclassified distribution
☐ 5. UC/C Category _____

☐ 6. Additional instructions/explanations _____

(Do not identify Sigma categories for Nuclear Weapons Data reports, and do not provide additional instructions that are inconsistent with C below.)

C. Recommendation *("X" at least one)*

☐ 1. Program/Standard Announcement/Distribution
  (Available to U.S. and foreign public)

☐ 2. Classified *(Standard Announcement only)*
☐ 3. Special Handling *(Legal basis must be noted below.)*
  ☐ a. Unclassified Controlled Nuclear Information (UCNI)
  ☐ b. Export Control/ITAR/EAR
  ☐ c. Temporary hold pending patent review
  ☐ d. Translations of copyrighted material
  ☐ e. Small Business Innovation Research (SBIR)
  ☐ f. Commercializable information
    ☐ (1) Proprietary
    ☐ (2) Protected CRADA information
      Release date __/__/__
    ☐ (3) Other *(explain)* _____

☐ 4. Program Directed Special Handling *(copy attached)*

D. Releasing Official

A. Patent Clearance *("X" one)*
  ☐ Has been submitted for DOE patent clearance
  ☐ DOE patent clearance has been granted

B. Released by
  (Name) _____
  (Signature) _____
  (Phone) _____
  (Date) _____

Purpose: This form provides the Office of Scientific and Technical Information (OSTI), AD-21, the data elements required to accurately process and/or announce and disseminate the result of work funded by the U.S. Department of Energy (DOE) or performed in DOE facilities.

When to use: Submit this form with each Scientific and Technical Information (STI) product/report title. When submitting electronically, include all relevant data elements, and prior to submission contact AD-21 at 615-576-1261.

1. DOE and DOE Contractors: Complete the entire form and submit with the STI product to AD-21 (OSTI) for processing in accordance with the requirements of DOE 1430.1C and 1430.2B. Reporting that may be required under the terms of the contract but is not appropriate for transmittal to AD-21 includes such things as contract proposals, funding status, routine construction or inventory reports, etc.*(Call 615-576-1261 for further clarification.)* Submit to:

> U.S. Department of Energy
> Office of Scientific and Technical Information (AD-21)
> l75 Oak Ridge Turnpike *(for shipments)*
> P.O. Box 62 *(for mail)*
> Oak Ridge, TN 37831

2. Financial Assistance Recipients: Normally, only Part I is to be completed. When completed, forward the form along with the STI product/report to the DOE Contracting Officer who will complete Part II and submit the package to AD-21. However, the DOE Contracting Officer may require the awardee to complete portions of Part II and also may require that the form and product/report be forwarded directly to AD-21. Check your specific requirements.

PART I

A. Product/Report Data
1. Contract (Award) No. Insert the DOE award or contract number(s) under which the work was funded.

2. Title. Provide the title exactly as on the product itself.

3.a., 3.b. and, 3.d. Self-explanatory.

3.c. Software. STI software must be submitted to the Energy Science and Technology Software Center (ESTSC). To obtain required forms and instructions, contact ESTSC at 615-576-2606.

B. Patent Information. Self-explanatory.

C. Contact. Self-explanatory.

PART II

A. DOE Identifiers
1. Product/Report Number. This is a unique identifier. A complete and accurate number is essential. AD-21 has approved identifiers for use by most DOE offices and Management and Operating (M&O) Contractors *(see examples below).* For others, use DOE/ and the final seven characters from the applicable contract or grant number. A slash mark must separate the letters from the number. Complete the number with dashes followed by a sequential number for each product/report generated under the contract. For example, the first product/report number generated under contract number DE-AC03-79NE01834 should have the number DOE/NE/01834--1. The following are examples of format for multivolumes, parts, or revisions.

> DOE/NE/01834--1-Vol. 1
> DOE/NE/01834--1-Pt. 1
> DOE/NE/01834--1-Rev. 1

Product/Report numbers are to be structured exactly as specified in these instructions. Any modification must be approved by AD-21. The following are examples of approved identifiers.

Product Producer	Approved Sequential Identifier
Headquarters DOE	DOE/NE--193
DOE Field Offices	DOE/OR--759
Major Project Offices	DOE/LLW--198
M&O Contractors	ANL/TM--482

For work performed for other agencies, the funding agency may assign their product/report number. If so, provide their number.

2. Funding Office. This information is essential. Insert the name, symbol, or B&R code of the DOE office providing support/funding. For projects funded by more than one office, indicate all sources of DOE funding. For work for others, indicate funding agency.

B. Copies for Transmittal to AD-21 (OSTI)
All STI products must be in a form that can serve as the record copy and be of sufficient quality for successful reproduction (optical scanning, microfiche, and other media). For nonprint media, refer questions to AD-21 at 615-576-1268.

1. and 3. For printed products, one copy must be original ribbon or offset and be completely legible according to DOE 1430.2B. A high-contrast photocopy is acceptable as a second reproducible copy.

2. and 4. When submitting print copies for distribution by AD-21, forward the number of copies specified in DOE/OSTI--3679-Rev. 75 or DOE/OSTI--4500.

5. UC/C Category This code identifies the appropriate distribution of the product/report. Provide the appropriate unclassified code from DOE/OSTI--4500 or classified code from DOE/OSTI--3679-Rev.75. For copies of these documents contact AD-21 at 615-576-8401.

6. Provide sufficient instructions for AD-21 to accurately process, announce, or distribute the STI product. Include complete funding information when requesting services. Use this block to note when mailing labels are included.

C. Recommendation
DOE is obligated to make available the results from federally funded work to the widest extent possible. AD-21 makes distribution of STI products on behalf of DOE strictly in accordance with existing laws, regulations, and/or written DOE Program Office guidance. Recommendations to restrict access to STI products must have a legal basis or be accompanied by written programmatic guidance. Questions concerning current laws and guidance may be referred to AD-21 at 615-576-1268.

1. Program/Standard Announcement/Distribution. The unrestricted, unlimited distribution of the product includes abstracting in *Energy Research Abstracts (ERA)*, DOE distribution to appropriate addressees listed in DOE/OSTI--4500, to those Government Printing Office (GPO) Depository Libraries maintaining energy collections, and to the National Technical Information Service (NTIS) for sale to the U.S. and foreign public.

2. Classified. STI products will be announced by AD-21 in accordance with DOE/OSTI--3679-Rev. 75.

3. Special Handling. The specific legal basis for restricting access must be checked. All STI products will be announced/distributed strictly in accordance with existing laws, regulations, or official guidance.

CRADAs—STI products generated under Cooperative Research and Development Agreements (CRADAs) . National Competitiveness and Technology Transfer Act of 1989. , aue include the estimated release date for the STI product in accordance with the terms of the agreement.

4. Program Directed. A copy of the specific guidance (or if the guidance is lengthy, a reference will be acceptable) must be attached.

D. Releasing Official
The appropriate official differs based on the source of STI, the contracting instrument, and the internal organizational responsibilities. Do not forward this form to AD-21 until after appropriate review and release.

OMB BURDEN DISCLOSURE STATEMENT
Public reporting burden for this collection of information is estimated to average 5 minutes per response, including the time for reviewing instructions searching existing data sources, gathering and maintaining the data needed, and completing and reviewing the collection of information. Send comments regarding this burden estimate or any other aspect of this collection of information, including suggestions for reducing this burden, to the Office of Information Resources Management, AD-244-GTN, Paperwork Reduction Project (1910-1400), U.S. Department of Energy, Washington, DC 20585; and to the Office of Management and Budget (OMB), Paperwork Reduction Project (1910-1400), Washington, DC 20503.

Table I. Economic Analysis Ceramic Anode Implementation

	1997	1998	1999	2000	2001	2002	2003	2004	2005	2006	2007
Production Mix											
Mag Produced with Graphite Anodes	100%	100%	90%	90%	75%	75%	50%	25%	0%	0%	0%
Mag Produced with Ceramic Anodes	0%	0%	10%	10%	25%	25%	50%	75%	100%	100%	100%
Costs											
Manufacturing MFG (M$)											
Anode Cost	0	0	0	0	0	0	0	0	0	0	0
Utilities & Operating Labor	0	0	-2,070	-2,070	-5,280	-5,280	-10,560	-14,235	-21,015	-21,015	-21,015
Depreciation	80	100	260	0	40	0	40	40	0	0	0
TOTAL MFG COST DELTA	80	100	-1,810	-2,070	-5,240	-5,280	-10,520	-14,195	-21,015	-21,015	-21,015
Capital											
Fixed (M$)											
R&D - Small	150	150	150	0	0	0	0	0	0	0	0
MFG - Small	50	100	500	0	100	0	100	100	0	0	0
Total Fixed Capital Delta	200	250	650	0	100	0	100	100	0	0	0
Book ValueDelta (M$)	200	250	640	640	700	700	760	820	820	820	820
Cash Flow Delta Summary											
Profit Before Tax (PBT)	-80	-100	1810	2070	5240	5280	10520	14195	21015	21015	21015
Tax	-30	-38	688	787	1991	2006	3998	5394	7986	7986	7986
Profit After Tax (NOPAT)	-50	-62	1122	1283	3249	3274	6522	8801	13029	13029	13029
Annual Cash Flow	-170	-212	732	1283	3189	3274	6462	8741	13029	13029	13029
Cumulative Cash Flow	-170	-212	520	1283	4472	7746	14208	22949	35978	49008	62037
Economic Profit	-71	-88	1055	1216	3175	3200	6443	8715	12943	12943	12943
Cumulative Economic Profit	-71	-88	967	2183	5358	8558	15001	23716	36659	49602	62545
Annual NPV Delta	-161	-201	694	1,217	3,023	3,104	6,127	8,287	12,353	12,353	12,353
Cumulative NPV Delta	-161	-201	493	1,710	4,733	7,837	13,964	22,252	34,605	46,959	59,312

8

More information can be extracted from this model by performing a sensitivity analysis. The following model variables are explored in the sensitivity analysis:

- 1/2 cent kW-hr increase in cost of electricity
- 1/2 cent kW-hr decrease in cost of electricity
- 10% improvement in electrical performance with respect to graphite anodes
- 10% reduction in electrical performance with respect to graphite anodes
- 10% decrease in replacement anode price
- 10% increase in replacement anode price
- Loss of Government funding for Phase III

The impact of these variables on the annual profit and the cumulative net present value after ten years is presented in figures 1 and 2.
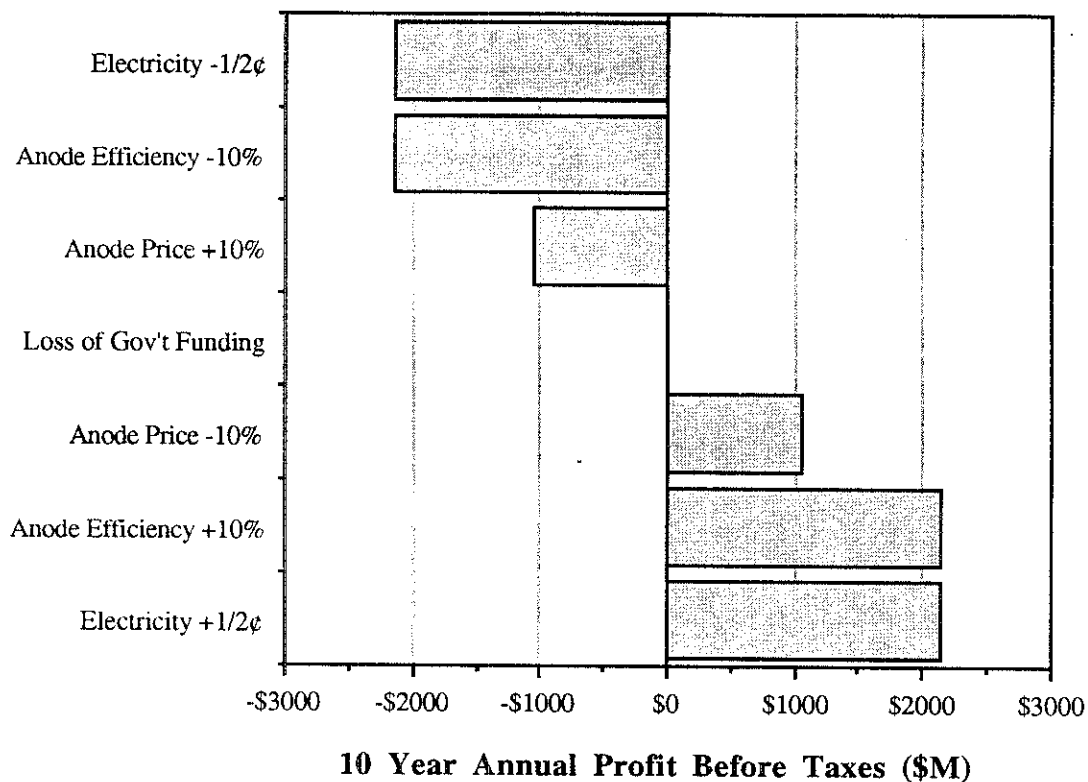

10 Year Annual Profit Before Taxes ($M)

Figure 1, 10 year charge in annual profit before taxes sensitivity analysis.
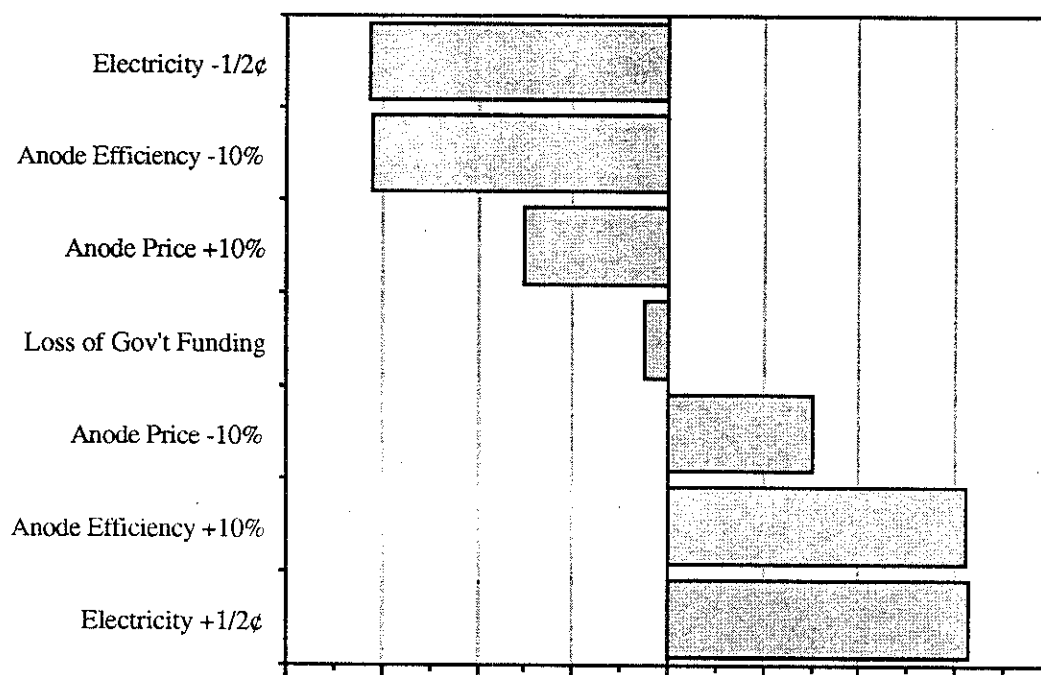
Figure 2, 10 year charge in cumulative NPV sensitivity analysis.

The two figures reveal that the change in cost of electricity and change in the electrical efficiency of the ceramic anode have the largest impact on both cumulative net present value and profit before taxes. The smallest impact on these economic indicators was the loss of Government funding for Phase III of the cooperative agreement. This small number arises from the analysis being evaluated at the 10 year interval which has the effect of de-emphasizing initial capital costs associated with the project implementation.

Ceramic Shell Development

The concept of making a dimensionally stable anode for magnesium production has a long history at the Dow Chemical Company[1]. The initial research performed on this technology identified some key issues faced by a ceramic anode. The first stems from the fact that most ceramics are electrically insulating. Obviously, for an electrolytic application such as used in magnesium production, this severely limits the choice of ceramic to one that has some electrical carrying capability. Even the most electrically conductive ceramics are simply not electrically efficient enough to be used as a electrode. Thus, a ceramic closed-

1 0

end tube must be fabricated and then filled with a highly conducting core to make an effective dimensionally stable anode. For the ceramic portion of this anode, the initial work performed by Dow Chemical identified titanium dioxide doped with tantalum pentoxide as a material that has both corrosion resistance to the molten salts in the magnesium electrolytic process and acceptable electrical semiconductivity. However, this initial research ran into insurmountable fabrication challenges when making the ceramic shell and then filling the shell with a conductive core. These fabrication problems, specifically the cracking of the ceramic shell, led to the work being discontinued. It is believed that the application of contemporary ceramic science and engineering methodologies can overcome these difficulties.

The initial ceramic anode research focused on isopressing a closed end ceramic tube. This process resulted in a ceramic article that had numerous flaws that were then exploited to cause failure when tested in the magnesium electrolytic process. The approach that this research takes is to "slip cast" the ceramic part. Slip casting is a ceramic forming process that is nicely suited to the production of thin walled ceramic parts and also is relatively easy to scale-up to production sizes.

Slip Casting

Slip casting is a classic ceramic forming process. The basic slip casting process has just a few steps. The first step is to suspend the ceramic particles in a liquid medium (most often water). This ceramic/liquid mixture is called the 'slip'. From a simplified view, the more stable the slip is the more uniform and flaw free the resultant ceramic part will be. This slip is then carefully poured into a properly prepared plaster mold. A lot of the 'art' of slip casting deals with the plaster mold preparation and can dramatically increase or decrease the quality of the resultant ceramic part. The plaster mold has a certain degree of porosity that is one of the mold making design variables that directly effect the ceramic part's casting time, density gradients, and surface texture. This porosity serves to draw the water out of the slip leaving behind a 'cake' on the plaster wall. When this cake gets to a designated thickness, the remaining slip is pour out of the mold. The cake is then allowed to dry in a very controlled manner to avoid any cracking of the cake. This cake is then removed from the plaster mold and dried further. This dried slip cast cake is called 'greenware'. This greenware can then be sintered or densified into a hard, dense ceramic part. Figure 3 shows a sketch of the slip casting mold used in casting the laboratory scale ceramic anode.
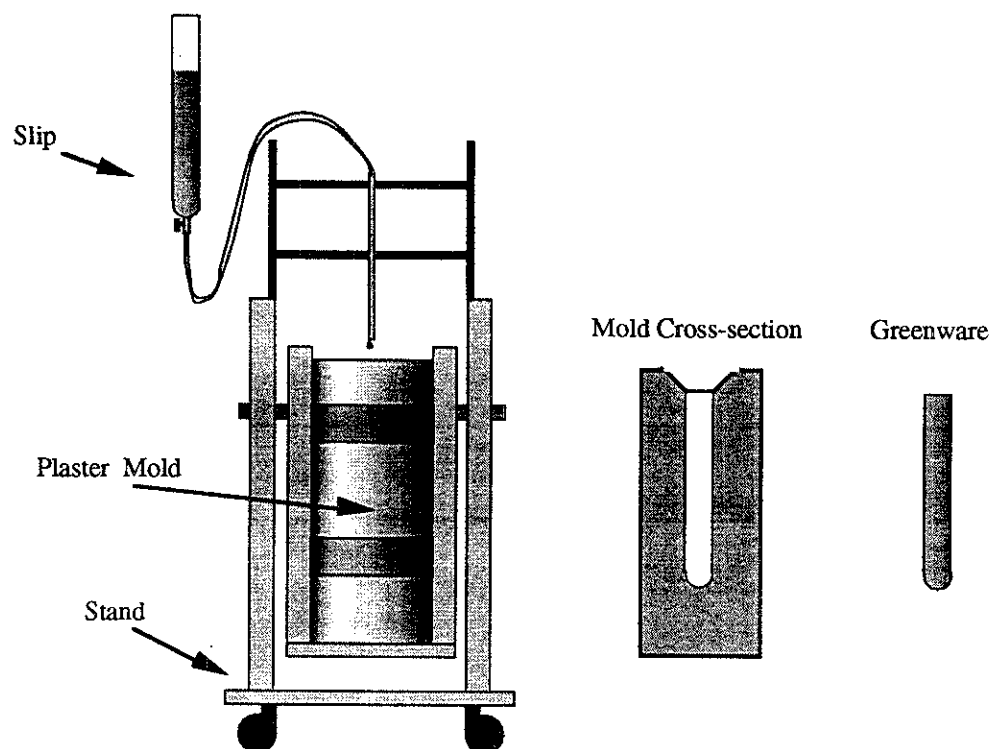
Figure 3, Sketch of the slip casting mold used in casting the laboratory scale ceramic anode

The following sections describe the particulars of identifying the raw materials, slip formulation and optimization, and sintering of the laboratory scale ceramic anode.

Raw Materials

The criteria for selecting the raw materials for fabricating the ceramic shell were as follows:

- Corrosion resistance to the magnesium cells molten salt environment.
- Electrical properties (electrically conducting or semiconducting)
- Available in commercial quantities.
- High in purity ($\geq 99.5\%$).
- Suitable for use in the process of slip casting of greenware in gypsum plaster molds.

In Dow's earlier research into dimensionally stable ceramic anodes, numerous ceramic materials were tested for corrosion resistance to the magnesium cells molten salt environment and electrical conductivity[1]. The results of this study showed that titanium dioxide (TiO_2) had good corrosion resistance, but more importantly, became electrically semiconducting when doped with 1-5 mole % tantalum pentoxide (Ta_2O_5). This doped titanium dioxide was used in Phase I and part

of Phase II of the cooperative agreement. However, a preliminary economic analysis pointed out that the high cost of tantalum pentoxide, even at the low doping levels, would add considerably to the cost of the final anode. Niobium pentoxide (Nb_2O_5) was identified as a potential replacement for tantalum pentoxide due to its similar electronic valence characteristics and also it's significantly lower cost on a molar basis. When Nb_2O_5 was used as a dopant to titania, it was found that the resultant ceramic material was also semiconducting with a very similar if not slightly more conducting in nature. Thus, the change was made with Nb_2O_5 replacing Ta_2O_5 as the minor component of the ceramic used for the ceramic shell.

Titanium dioxide (titania) meets the third criteria with its wide commercial use base. The major uses for titania is as a pigment in products such as paints, plastics and pharmaceuticals. These pigments often have additives. Since titania is the major component of the semiconducting material that is doped with either the Ta_2O_5 or Nb_2O_5 material, the availability of titania is the dominant factor.

The TiO_2 selected having the needed purity was from TAM Ceramics, Inc. and is their TICON™ grade HP 59030. The Ta_2O_5 powder selected was from Hermann C. Starck Berlin, and is their standard optical grade. The Nb_2O_5 powder selected was from Kronos, inc. and is their high purity, ceramic grade.

All of the materials selected meet the third and forth criteria listed above. In the next section are described the procedures used to make them meet the fifth one. The titania is within the "typical properties" as listed by the supplier for surface area but the particle size, based on the D_{50}, is somewhat higher than the top of the 1-5 μm range listed. Starck's tantalum pentoxide is supplied with a nominal particle size of 90% minus 325 mesh (44 μm) and is somewhat larger than that with a measured D_{90} of 50 μm. Its surface area is low as expected with the large particle size. The Kronos material has a very similar size distribution to the Starck material. All of the materials are too large in particle size to make good casting slips without grinding to a $D_{90} \leq 2$ μm.

Slip Preparation

Dispersion of the powder within a slip is critical to the uniformity to the resultant ceramic part. Dispersion response was examined by measuring the viscosity as a function of surfactant addition (deflocculation curves). The viscosity was measured with a Brookfield rotating disc viscometer. The slip pH was monitored during the surfactant addition. In addition, the slips were examined for any foaming while these deflocculation curves were being constructed.

Surfactant performance during attrition milling was examined by measuring the particle size distribution of a 40 volume % TiO_2 slip after 11 hours of attrition milling at

13

200 rpm. Due to the coarse nature of starting powder, a 40 volume % suspension could not be obtained (due to dilatant flow) prior to attrition milling. For this reason, the water was added to the attritor first, and the powder was added slowly while the attritor was running. The attrition mill size was 1 quart. The milling media was 5 mm yttria stabilized zirconia balls. The media was added in sufficient amount to just cover the top of the attritor blade. The formulation was sized so it was sufficient to just cover the media during attrition (≈ 350 ml). Further information on deflocculant performance during attrition was gained by measuring the Brookfield viscosity after removing the slip from the attrition mill.

Deflocculant requirements are:

1) Maximum powder dispersion.
2) Minimal degradation during attrition milling.
3) Deflocculate in mid to high pH range.
4) Low foaming.
5) Clean, efficient burnout.
6) Ammonium based (for conductivity requirements).

Requirement 2) is necessary because these powders must be attrition milled due to the coarseness of their particle size. Deflocculation in the mid to high pH range is preferable to reduce plaster mold wear. Ammonium based dispersants were used because they do not leave a cationic residue which is capable of affecting conductivity measurements. Requirements 1), 4), and 5) are standard for a normal slip casting operation.

Deflocculation curves similar to Figure 4 were constructed for a number of different dispersants. The performance of each of the surfactants is summarized in Table II. It can be seen from the table that Darvan C, Darvan 821A, and pH adjusted citric acid seem to promote good TiO_2 powder dispersion. Other dispersants either were not as powerful, or they dispersed in a low pH range and/or foamed substantially.

The Darvan C, Darvan 821A, and pH adjusted citric acid surfactant systems were selected for further evaluation based on their superior properties. It was found that the viscosity of the slips deflocculated with the Darvans were at least an order of magnitude greater than the slip dispersed with pH-adjusted citric acid. It was also seen by comparing the D90 values that the particle size distributions of the slips deflocculated with the Darvans were significantly coarser creating a less desirable slip than the slip deflocculated with pH adjusted citric acid.

14

Table II. Summary of Defllocculant Performance

| SURFACTANT	PERFORMANCE
Darvan C	Excellent, dispersed in mid pH range
Darvan 821 A	Excellent, dispersed in mid pH range
Colloid 111M	Excellent, but foamed substantially
Ammonium Citrate	Fair, dispersed in low pH range
Nalco CX2209	Good, but foamed substantially
Ammonium Hydroxide	Fair, dispersed in mid to high pH range
Citric Acid	Poor, low pH, did not disperse
pH-adjusted Citric Acid (NH4OH)	Excellent, dispersed in mid pH range
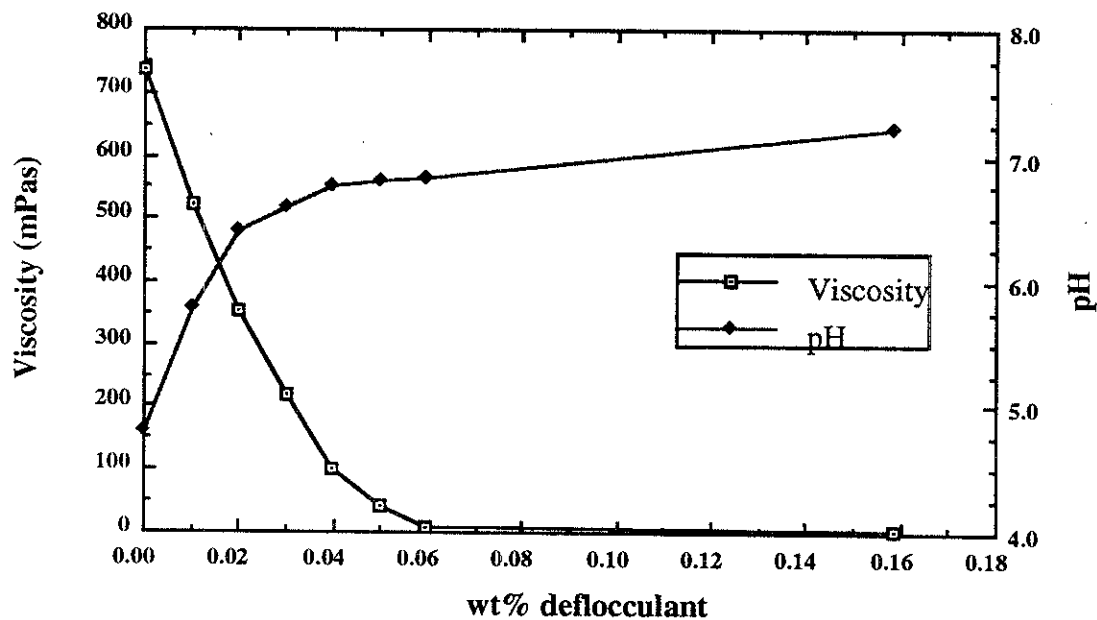
Figure 4, Deflocculation Response of TiO2 to Darvan 821A

The difference in particle size data from slips using different deflocculants can be explained by considering the values for viscosity. If a suspension becomes flocculated during attrition milling (as it is at higher viscosities), a significant percentage of the media impact energy will be used in breaking up flocs, thereby decreasing the available energy available for particle fracture. It seems as though the Darvan surfactants degrade during attrition milling. This behavior has been known to occur for high molecular weight surfactants. Also, the higher slip viscosities will affect the cast adversely by lowering the bulk density of the casting. Thus, pH-adjusted citric acid was used for most of the casting work performed in this program.

When the change was made from the tantalum doped titania slip to a Niobium slip, the deflocculant selection experiments where repeated. Figure 5 shows the difference in the viscosity between a tantalum and niobium doped slip. Both of these slips where dispersed using the pH corrected citric acid dispersant which was found to be preferred for the tantalum doped slip. This graph shows that the viscosity of the niobium doped slip is significantly less (approx. ~3 times) than the optimized tantalum slip. This reduction in viscosity presents an opportunity to improve the casting density and uniformity by increasing the solids loading of the slip.
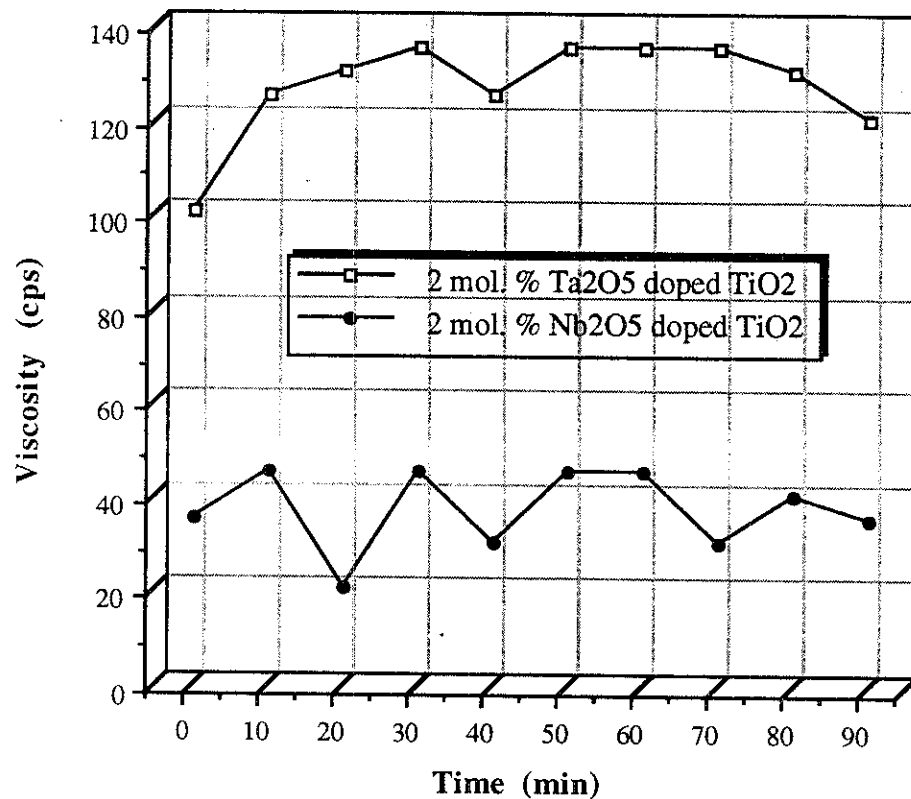

Figure 5, Viscosity difference between tantalum and niobium doped slip

A study was undertaken to evaluate the effect of solids loading on the viscosity. A 60 volume percent solids loaded slip was made making sure that it was milled to the correct particle size. This slip was then mixed with the standard 40 volume percent slip to arrive at the various loadings levels. After tumbling for 30 minutes, the viscosity was measured for

each slip. Two sets of data were taken for conformation. Figure 6 shows the data from this series of experiments.
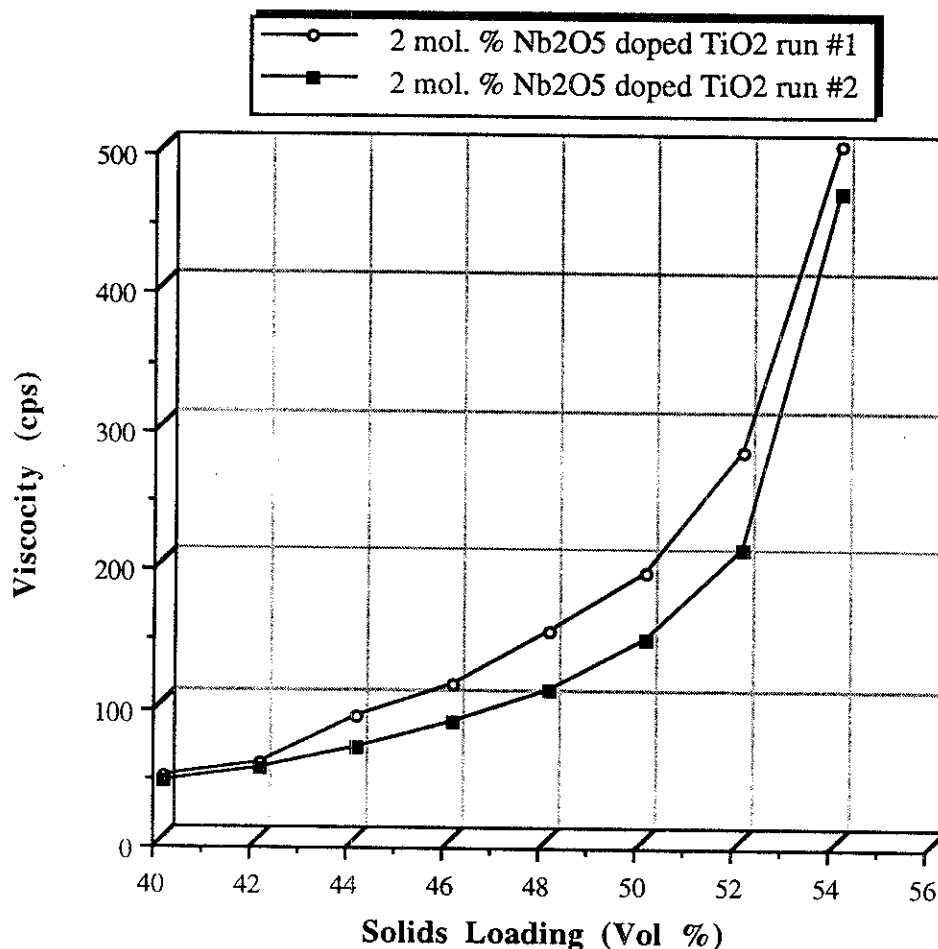

Figure 6, Effect of solids loading on slip viscosity

Based on these viscosity measurements, and the more qualitative observations on handlability of the slip, a solids loading of 48 % was chosen. This higher solids content results in higher cast greenware densities while also reducing the density gradients in the part.

Sintering

Prior studies[2-4] of sintering titania have shown high sintered density (≥ 97% of theoretical density) being achieved between firing temperatures of 900°C and 1550°C. Sintering shrinkage of titania and titania plus 1 to 5 mole percent tantalum pentoxide was studied using a

dilatometer (Theta Industries 1600°C system) with alumina holder and sensor rod. Titania (11 hr attrition) sintered for two hours at 1200°-1250°C in air yielded a very acceptable ≥99% dense ceramic. The higher temperature results in a more than doubling of the grain size which can adversely effect the strength of the ceramic.

Figure 7 is a plot of density vs temperature for titania heated at 5°C/min to 1200°C and held at that temperature for two hours. By immersion in water (Archimedean method) the bulk density was determined to be 99.0% of theoretical density (TD).
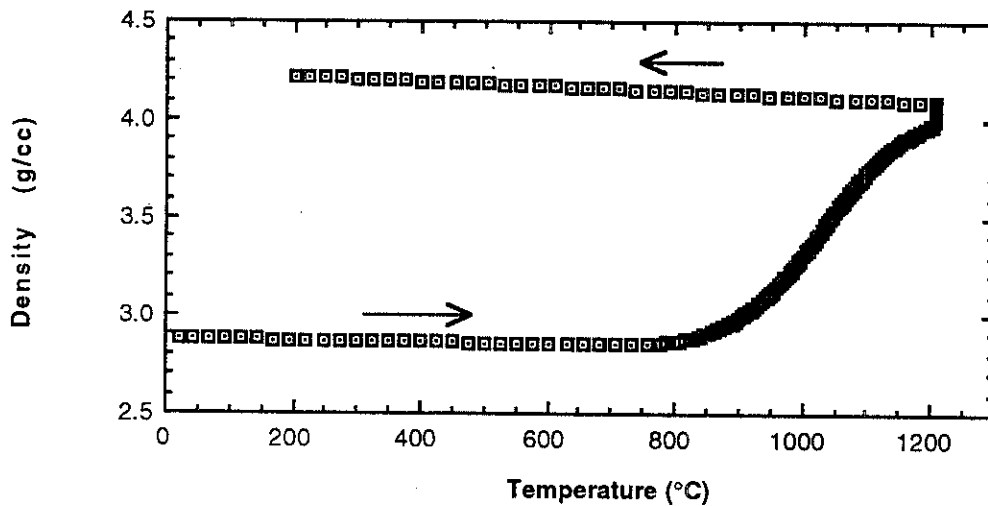

Figure 7, Density versus temperature for the sintering of pure titanium dioxide.

The average grain size was determined to be between 2-3 microns. Increasing the sintering temperature to 1250°C results in the larger grain size. The smaller grain size ceramic has the advantage of increased fracture strength and thermal shock resistance but has reduced electrical properties, due to grain boundary resistance, as compared to the larger grain size[4,5].

The slightly reduced final density of both the tantalum and niobium doped ceramics appear to be caused by a reaction taking place in the early stages of sintering. Figure 8 shows the grain structure of a 3 mole % Nb_2O_5 doped titanium dioxide ceramic sintered with a 3 hour hold at 1200°C. This ceramic had a final density of 97.6% of theoretical. The dark spots on the micrograph correspond to voids. These voids are located at the grain boundaries. By simply varying the sintering temperature and time, we were not able to reduce/eliminate these voids.

Figure 8, Microstructure of 3 mole % Nb_2O_5 doped titanium dioxide sintered at 1200°C for 3 hours.

It is thought that these voids are formed in the early stages of sintering as the Ta_2O_5 or Nb_2O_5 dopant begin to react with the titanium dioxide to form a solid solution. As the doping metal cations are integrated into the titanium dioxide rutile crystal structure, the excess oxygen is released. If not allowed to migrate out of the porous ceramic, this oxygen can be trapped at the grain boundaries inside the ceramic. To allow for the oxygen migration, a rest at the temperature where the porosity first was observed was included in the sintering schedule. A series of experiments resulted in developing a sintering schedule with a 1 hour hold at 1050°C and then a second hold for 2 hours at 1150°C. The final density for this doped ceramic was >99% of theoretical. Figure 9 shows a micrograph of this highly dense ceramic with minimal voids.
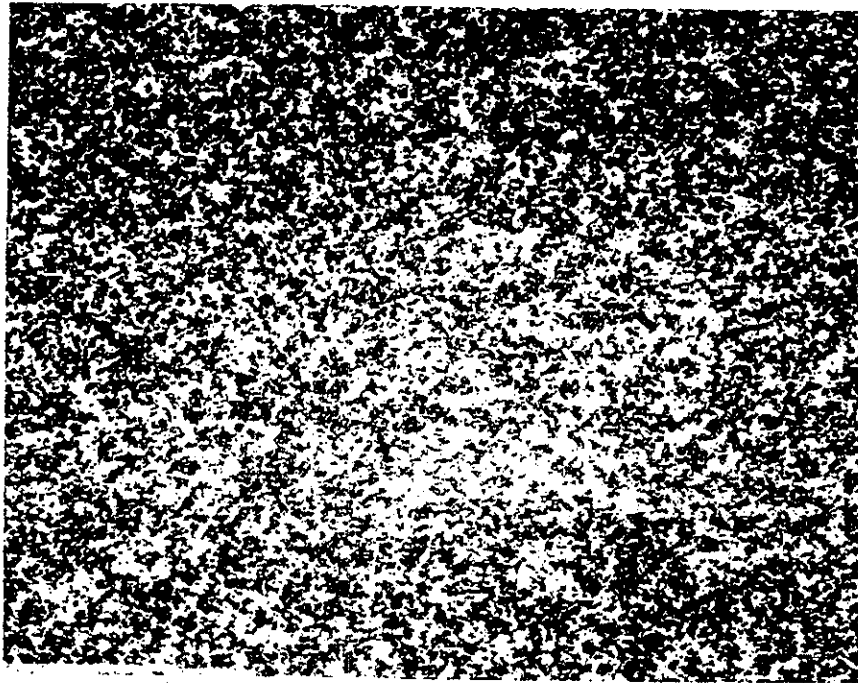
19

Figure 9, Microstructure of 3 mole % Nb_2O_5 doped titanium dioxide sintered using optimize schedule.

Ceramic Physical Characterization

Greenware disks were prepared by slip casting of a 95:5 mole ratio TiO_2:Ta_2O_5 for use in making flexural test bars. The disks were sintered for two hours at 1480°C. The disks were then sent out for machining into flexural strength test specimens (4.0mm x 3.0mm x 45 mm) suitable for "configuration B" as outlined in ASTM C 1161–90, "Standard Test Method for Flexural Strength of Advanced Ceramics at Ambient Temperature." Specimens were tested in the "four-point-$^1/_4$ point" configuration at room temperature and 800°C.

Young's modulus, bulk modulus, shear modulus, and Poisson's ratio were measured at ambient conditions with a sonic technique on each of the flexural strength specimens before breaking. The results of this testing and the flexural testing are in Table III.

The room temperature strength compares well with the literature[2] where average four-point bend was reported to be ~ 18 Ksi for 1 mole % Ta doped ceramics. The fact that we are above with reported strength value for similar materials is a good indication of the high quality of our ceramics.

Table III. Physical Property/Characteristic Values for Moduli and Flexural
Strength of Sintered 95/5 Mole % Titania/Tantalum Pentoxide
Greenware Prepared by Slip Casting.

PROPERTY/CHARACTERISTIC

DENSITY (gm/cc)	4.58
% DENSE	96
YOUNG'S MODULUS (psi x 10^{-6})	36
BULK MODULUS (psi x 10^{-6})	25
SHEAR MODULUS (psi x 10^{-6})	14

FLEXURAL STRENGTH (Ksi) @

Temperature (°C)	(Ksi)
23	26.0
800	20.0

One important trend to be noted from this table is the decrease in strength as a function of
temperature. This is significant due to the fact that the ambient temperature of the molten salt bath
used in magnesium electrolysis is 720°C. Thus, the operating strength of the ceramic is
significantly lower the room temperature strength.

Anode Assembly Development

The goal for assembly of a successful anode was to completely fill of a ceramic
shell with a highly conductive material without cracking the shell during the process. For
success, a core formulation must achieve a balance between the following :
1. Achieving good electrical and physical contact with the shell's inner surface.
2. Having sufficient electrical conductivity such that the assembled anode has
   electrical efficiently equal to or better than graphite anodes.
3. Having thermal expansion characteristics throughout the filling and subsequent
   thermal cycles such that neither the bond between the core and shell nor the
   ceramic shell itself will break.
In pursuit of fulfilling the above criteria, a variety of core materials and shell modifications
were investigated.

Core Material Identification

In order to meet the criteria for a solid core material, a ceramic - metal composite was pursued. The core material must be a strong electrical conductor while having a good thermal expansion match with the ceramic shell. Efforts to develop a suitable metal-ceramic core system for filling the ceramic shells are currently focused on the binary titanium (Ti) - copper (Cu) system for the metal component of the core material. Initially, additions of 2-9 weight % Ti were made to the Cu. Then silicon carbide (SiC) powders were combined with these alloys to reduce the thermal expansion of the alloy. Unfortunately, the titanium was found to react with the SiC. Titanium carbide was then obtained for use as the ceramic powder. The alloy composition was also shifted to the high titanium side (above Ti_2Cu). The liquids in this compositional area strongly wet both the ceramic and graphite.

A composite composition with 50 volume % TiC was prepared as a bar at 1100°C for thermal expansion measurement and comparison to the 5 mole % tantalum pentoxide doped, titanium dioxide ceramic shell material. Figure 10 shows the thermal expansion data for these anode components. The graph shows the linear thermal expansion coefficients versus temperature plots for a 62/38 weight % Ti/Cu alloy, the ceramic, and the composite. The liquidus temperature for this alloy is below 1100°. It was thought that the match between the ceramic and the composite were not as close as probably needed. Higher volume fraction ceramic composites were then attempted.

A first attempt was made at filling a shell with the 50 volume % TiC composite. The blended mix of Ti, Cu, and TiC powders was cold isostatically pressed as short cylinders. These were then hand abraded and inserted into a sintered shell. These filled the shell to within about an inch of its top and most of the diametrical space. For firing it was set vertically into a graphite support cylinder. This was placed into a vertical tube (fused quartz tube) furnace. A $3/4$ inch diameter graphite rod was set into the unfilled top of the shell. A cylinder of graphite (3 lb) slightly smaller in diameter than the furnace tube, with a center hole fitting over the rod, kept the rod aligned and applied a small load to the core. This assisted in consolidation of the composite core and pushing it against the wall of the shell. The graphite rod was pushed about one inch further down into the shell. Unfortunately, during this "filling" process, the rod was not kept aligned with the anode cracking the anode shell.
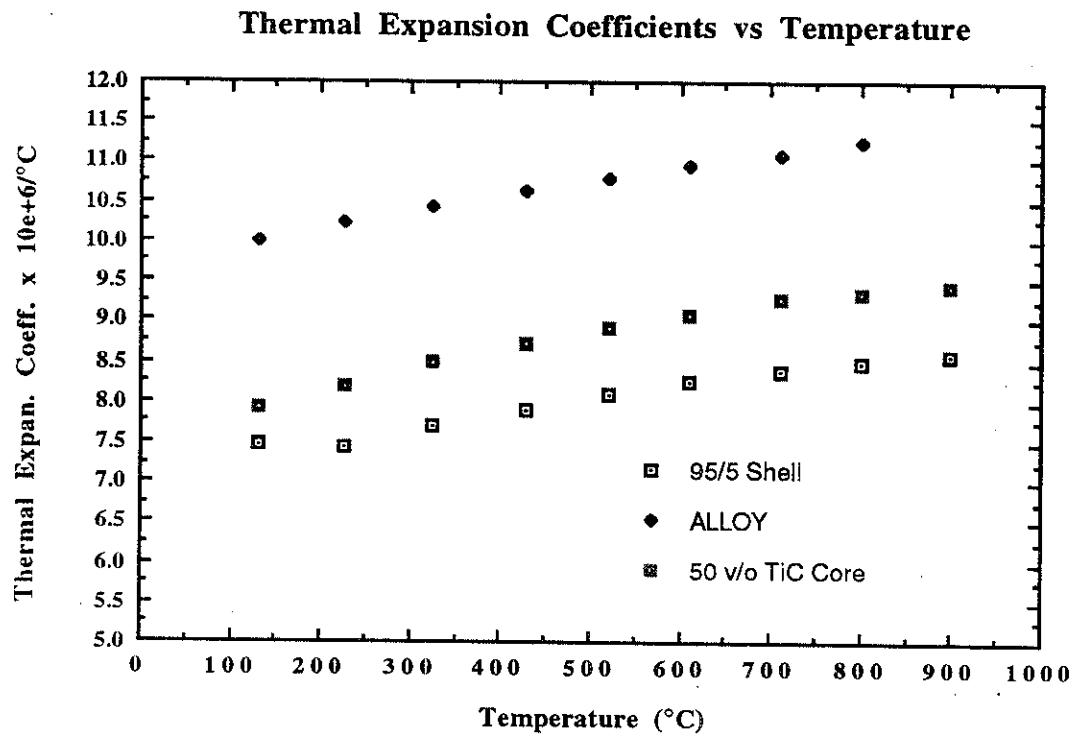
22

Thermal Expansion Coefficients vs Temperature

Figure 10, The thermal expansion data for the anode components

Thermal Expansion Characterization

Cracking of the ceramic shell proved to be a more refractory problem than expected from earlier modeling studies of the expected stresses in the anode. This led to a re-examination of the thermal expansion coefficient of our ceramic material. Previously, the ceramic tested was material that had only gone through the normal sintering cycle. New measurements were done on ceramic that was sintered and then run through the anode core filling process heating cycle. The results of this testing are shown in Figure 11 along with results for the ceramic after only the sintering. The filling cycle results in significantly lower thermal expansion. Figure 12 compares plots of sintered and heat treated ceramic with a composite core that we have used. These results indicate the thermal expansion mismatch and resultant stress must be much greater than previously recognized.

Knowing that the thermal expansion mismatch between the ceramic shell and composite is too great, new lower thermal expansion composites must be developed. Through differential scanning calorimetry, it was found that the alloy made from pure metals was not at phase equilibrium in the composite. Therefore, pre-alloyed material was obtained to ensure that the correct phases were being created. Higher ceramic component

23

formulations were also studied. A change in the alloy composition to allow incorporation of a lower expansion ceramic component was also considered.
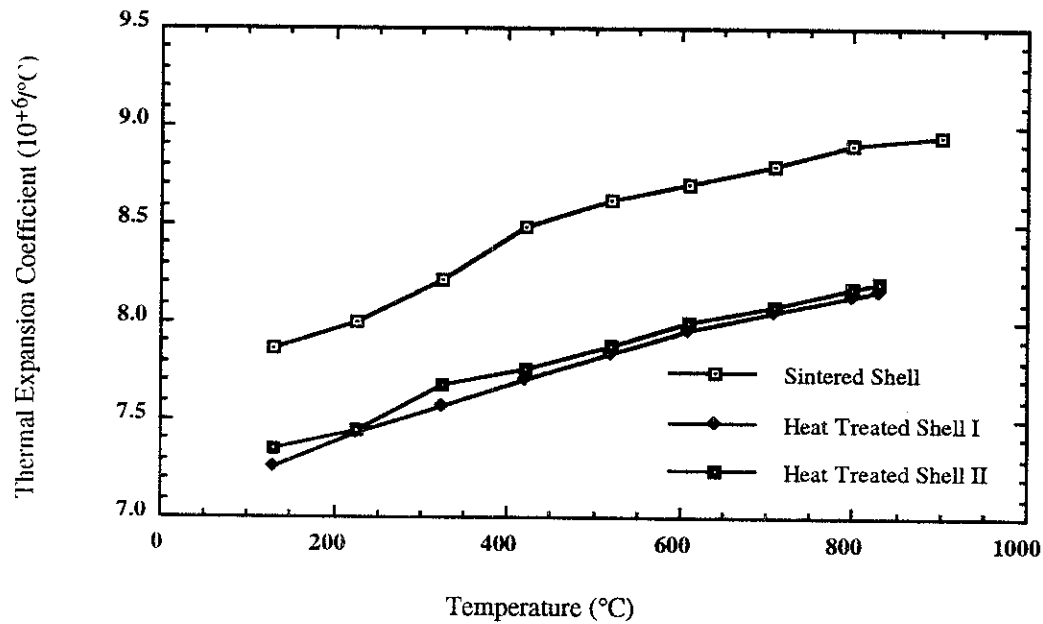

Figure 11, Effect of the thermal cycle in filling an anode on the thermal expansion coefficient of the ceramic.
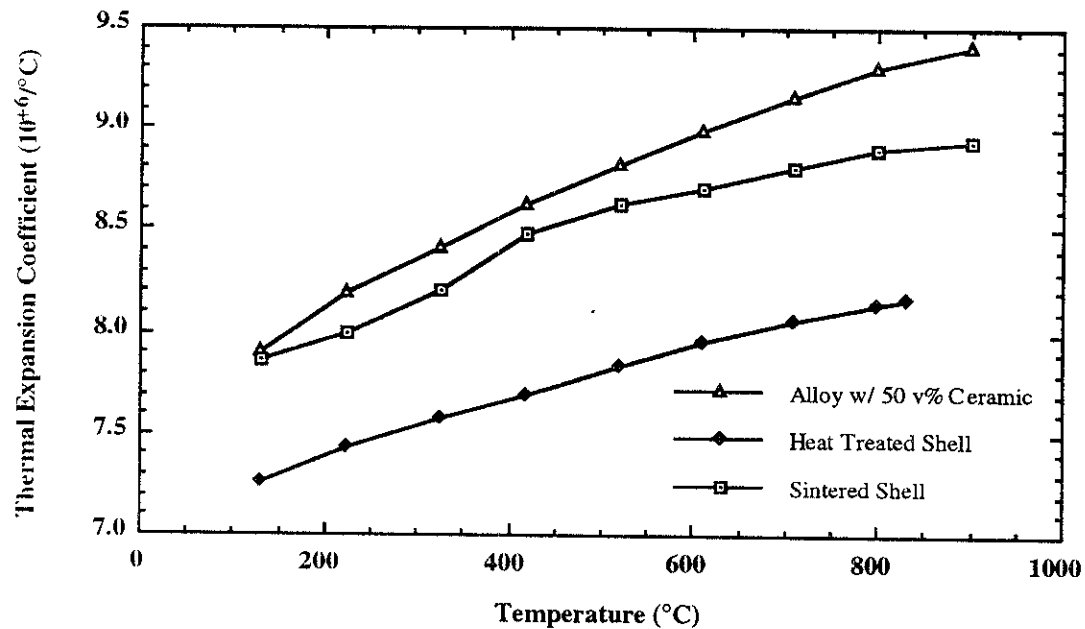

Figure 12, Comparison of thermal expansion coefficients of sintered and thermally cycled ceramic to core composite.

Finite Element Analysis Stress Modeling

24

The proposed structure of the ceramic anode requires proper matching of the coefficients of thermal expansion of the composite core material and the inert ceramic shell. A coupled dynamic heat transfer - thermal stress analysis modeling study was being used to provide design information on geometry and material composition for laboratory scale ceramic anodes. For performing the modeling calculations, the commercially available computer program, trade named ABAQUS, was used. ABAQUS is a robust finite element program capable of making dynamic heat transfer and thermal stress calculations for complex geometries. The program inputs are geometry, moduli, coefficients of thermal expansion, temperature dependent thermal conductivities and specific heats, and the thermal and physical boundary conditions. The plan called for making an initial set of calculations early in the research program using material properties found in our literature search for the proposed core composite components copper and silicon carbide.

The ceramic anode modeled is comprised of a titania shell with a current carrying Titanium carbide (TiC) ceramic/copper (Cu) metal composite core. Thermal stress modeling results on the lab scale anode, shown in Figure 6 for a specific titania shell thickness, reveals that the optimal core composition that results in the lowest thermal stresses is approximately a 50/50 volume ratio TiC/Cu composite composition.

The results also show that at higher percentages of SiC in the core composite, the thermal expansion mismatch and the increased modulus, or stiffness, of the core material results in increased tensile stress levels concentrated at the core-shell interface. Core materials with TiC component percentages less than 50% also experience increased tensile stresses but these are concentrated in the shell's rounded bottom area due to thermal expansion mismatch. These results point to pursuing the 50/50 TiC/Cu core composite to minimize thermal tensile stresses.

Simulations have also been performed on the potentially more severe, transient stress evolution that occurs in actual operation of the magnesium cell as the anode is initially placed into the reactor. Results from this simulation have shown that the optimized 50/50 TiC/Cu composite core anode design should survive the predicted transient thermal stress levels. Thus the results of these calculations on the lab scale anodes indicate that they should have little problem surviving the thermal stresses during any phase of operation testing.

25

Anode Fabrication

More recent efforts to fill the ceramic shell with the composite core were done with a support, load application apparatus. The apparatus or filling stand is shown in Figure 13. This stand eliminates the alignment problem and also increases the filling load that can be applied. The stand is made from stainless steel. The force of the weights is applied to the core by the graphite ram. Complete filling of the shell by the core has proven difficult.
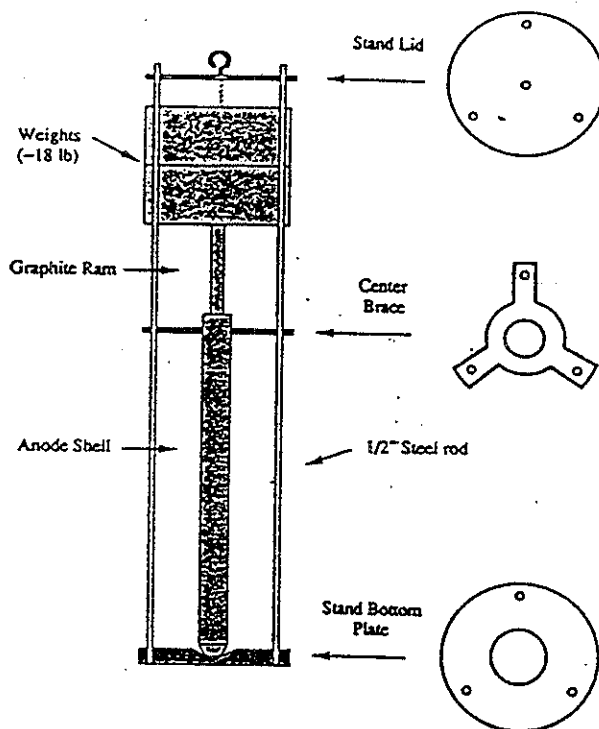

Figure 13, Furnace stand for filling laboratory scale anodes.

Based on computer modeling of this anode, it was evident that the magnitude of the hoop stress in the anode when cooled to room temperature would be near the critical stress. Physically, any cracking would be attributed to the thermal contraction of the graphite being less than the shell-core system. Experimental results show the tensile hoop stress exceeds the strength of the material surrounding the graphite rod in most cases. This results in the formation of cracks in the composite and shell along the length of the anode. In 6 of the 8 runs cracks originating out from the graphite-core interface and propagating through the ceramic shells were formed.

Stainless steel rods, also a half inch in diameter and varied in length from 9.5 to 10.5 inches, were next tried as the ram. These have thermal contraction greater than the core and shell. The steel's higher thermal contraction should load the core and shell into compressive stress after the alloy of the core solidifies and will no longer plastically

deform. Though not yet confirmed through modeling, it appears the shear strength of the ceramic shell is exceeded. Cracking of the ceramic shell occurred in 5 experiments with stainless steel as the ram. The composite core successfully withstands the stress on it. The results suggest the bond between the shell and core is strong enough to transfer sufficient stress to the shell to cause the shell to fracture.

One of these stainless steel rod runs came very close to completely filling the cavity of the shell. Most of the ceramic had to be removed with a hammer. Filling is estimated to have been about 99 volume %. The stainless steel rod and core are shown in Figure 8.

Because of cracking, the solid stainless steel rods were abandoned for hollow half inch outside diameter stainless steel tubes. With this change it was hoped the stainless steel would yield rather than cracking the ceramic in cooling. However, the tubes were not sufficiently rigid at the necessary temperature and they bowed or buckled and either did not go in centered or did not go in far enough.

Finally, cast gray iron half inch diameter rods were tried because cast iron has thermal expansion closer to the shell and core than any of the previously tried materials. Unfortunately, cast iron softens too much at the filling temperature and resulted in the same types of failure as the hollow stainless steel tubes.

Pre-densified SHS Core Material

The core material is a combination of metal components (alloy) and a ceramic component. The former are used for their electrical/thermal conductivities and the latter is used for its thermal expansion reduction. Prior work had been with metal powders (not alloyed) and a ceramic powder blended together to achieve an alloy-ceramic composite. The blended powders were cold pressed and shaped to fit inside the ceramic shell. The loaded shell was set, with a push rod in the top, in the furnace stand[5]. The furnace stand holds the shell and push rod in alignment vertically while a load is applied during the thermal cycle. As the metals alloy and melt, the load pushes the composite (consistency believed to be like wet sand) down into the shell. When the composite has been rich enough in liquid to flow sufficiently to fill the cavity, the thermal expansion has been too high and the shell has cracked in cooling. Reducing the alloy (or liquid) content results in an incompletely filled shell.

A new approach to the core material is preparation of predensified granules of a composite composition. A unique processing method using self-propagating high-temperature synthesis (SHS) to prepare these densified granules has been developed. This method has overcome phase segregation problems encountered using conventional

2 7

methods. The SHS process involves the exothermic self-sustaining reaction of a powder charge into a homogeneous powder compact or a dense ceramic body. The powder charge is packed into a crucible where a resistively heated tungsten filament ignites an exothermic reaction converting, in this case, the titanium, carbon, and copper powder mixture into homogeneous, titanium carbide reinforced titanium/copper alloy cermet. Figure 14 presents a schematic of this process. The resultant product is a porous cake. This porous cake is then crushed into 1-3 mm granules. Using these granules as a fill material with our conventional core filling procedures results in a uniform filling of the shell with a uniformly porous core. Figure 15 is a sketch showing the anode design using the SHS predensified core material. Radiographs (gamma ray exposure) of filled anodes indicate achievement of good contact, i.e. filling, at the core-shell interface. To improve the electrical properties of the anode using the SHS core material, minor additions (~10 wt. %) of titanium/copper alloy powder are mixed with the SHS granules before being used in the filling process. Anodes fabricated with this method have improved electrical properties, as shown by resistivity measurements on filled anodes.

Dilatometer studies of linear thermal expansion, see Figure 16, show a reasonable match of these new core materials with the ceramic after it has had the thermal treatment of the filling cycle (the filled circles). The porosity of the SHS material has the added affect of reducing the modulus of the core. By reducing the modulus (or stiffness) of the core material, any stresses generated by the thermal expansion mismatch between the core and the shell are partially alleviated by the core's ability to deform and not transmit the stresses to the fragile ceramic shell.

Tungsten
Ignition Coil

Product
TiC + nTiCu Alloy

Insulated
Platform

Combustion Front
Ti + C -> TiC
$\Delta H_{RXN} = -184$ kJ
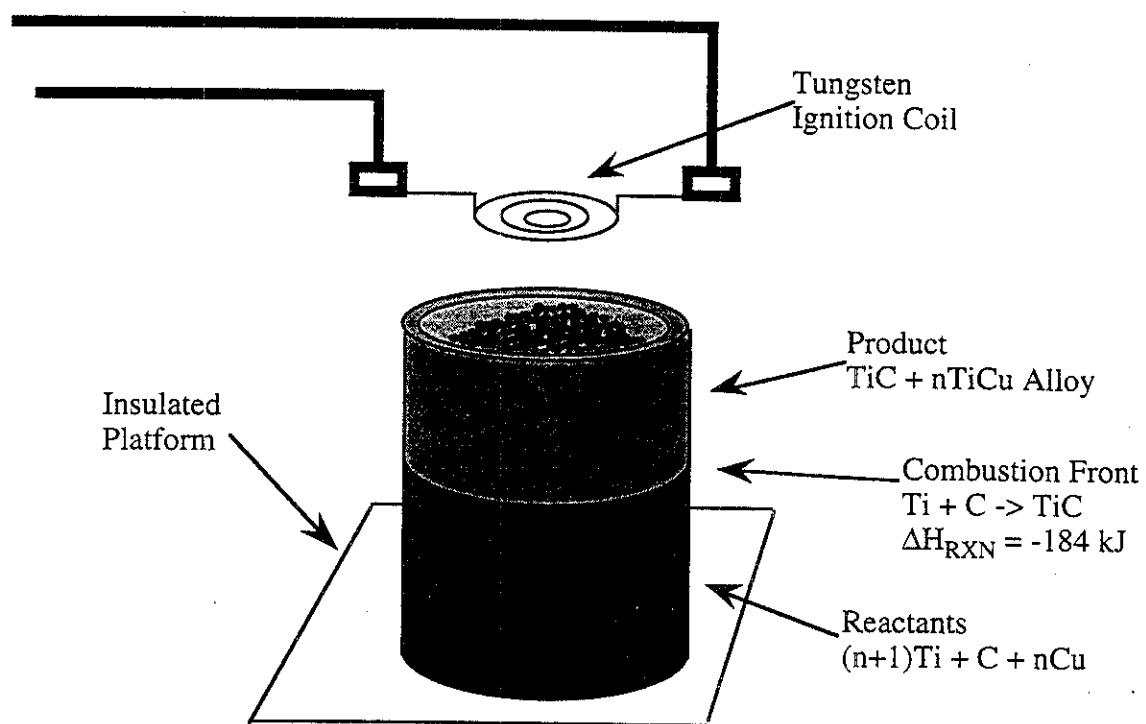
Reactants
$(n+1)Ti + C + nCu$

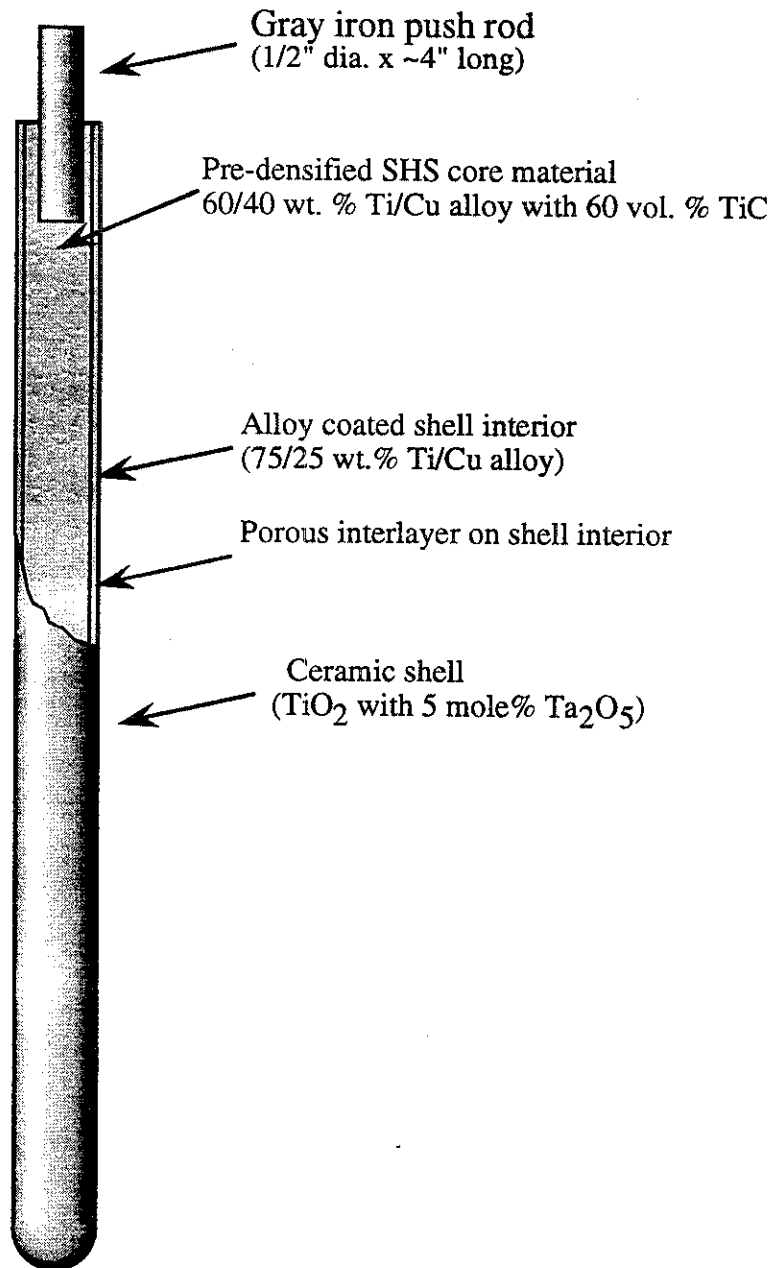Figure 14. Schematic view of an SHS reaction

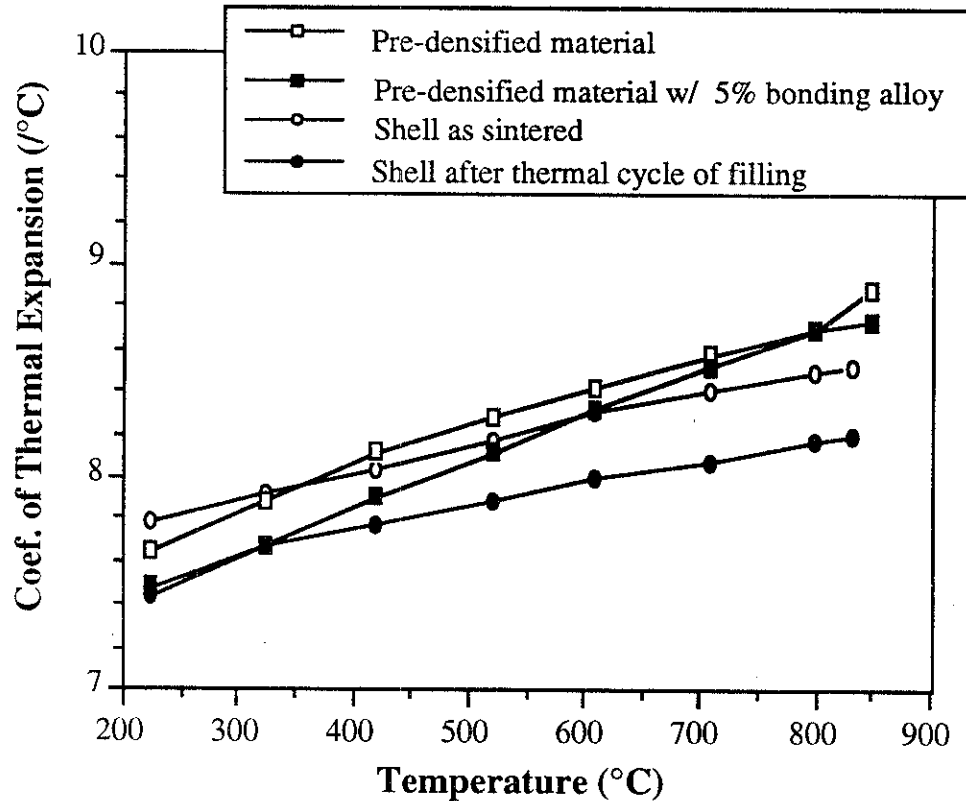Figure 15. Sketch of a lab scale anode using the SHS core material

Figure 16, Thermal expansion coefficients of shell and core materials.

Bonding of Shell and Core

The inner surface of a typical sintered ceramic anode shell is very dense and smooth, like a mirror. This has made the chore of developing a physical or interlock bonding between the core and shell. The bond is important for both good electrical conduction and physical strength. After failing in attempts to develop a chemically modified interlayer, work has been directed at roughening the inner surface with the hope of producing some degree of interlocking structure at the interface. Chemical etching, other than with strong hydrofluoric acid, proved unsatisfactory. Use of hydrofluoric acid was not continued because of safety concerns.

Success has been achieved in making a surface providing porosity for the liquid portion of the core to penetrate and interlock. Figure 17 shows photomicrographs of anode shell inner surface cross-sections. The upper photo (as fractured cross-section) is of the normal dense surface and the lower photo (fractured and polished cross-section) is of the porous rough surface. Work is in progress to minimize the thickness of the porous interlayer and to test with the core system to determine the penetration into and bonding to the interlayer.
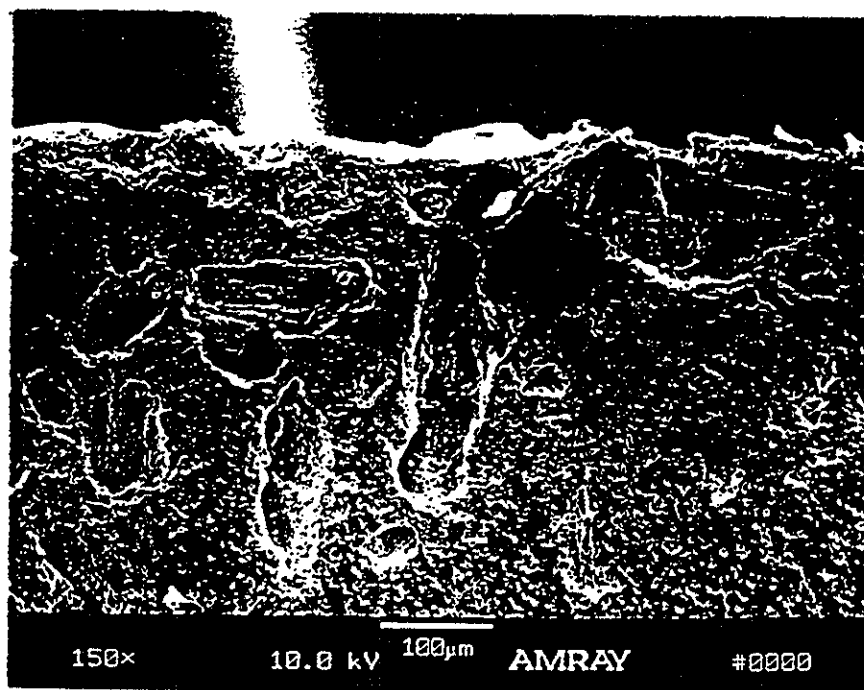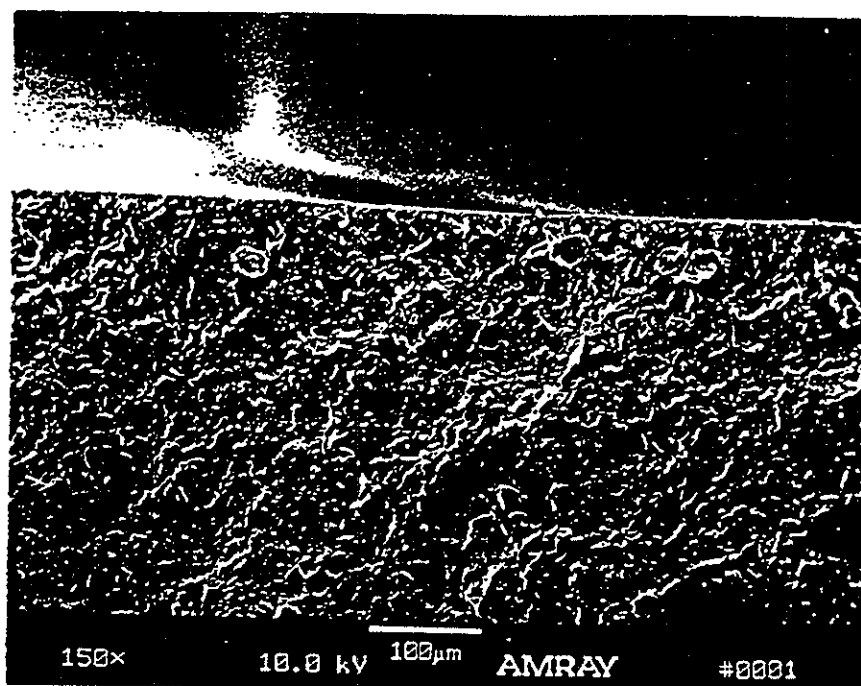
Figure 17. Photomicrographs of cross-sections of sintered anode shells with and without porosity to enhance core/shell bonding.

Alloy Precoating

In filling the anode shell with predensified granules, contact between the shell and core material is limited by the porous structure. To improve electrical performance, a coating of alloy is applied to the inner surface of the ceramic and thermally treated to bond. This is referred to as "Shell's precoated porous interior surface" in Figure 15.

Electrical Performance Optimization

The reduced modulus and the improved filling characteristics of the pre-densified core material permits a wide range of material and design variations to be investigated without jeopardizing the physical integrity of the anode. The benefits from this unexpected design flexibility were explored through anode design iterations.

The high porosity (~50%) of this core material has the benefit of a lower elastic modulus. The elastic modulus, or material stiffness, reduces the stress carrying ability of the composite core. Thus, a larger thermal expansion mismatch between the core and the shell can be tolerated without cracking the shell. This opens the door to a wide range of design and material development. The porosity of the system will also allow the anode to meet the weight requirements for full scale operational testing.

The significantly reduced shrinkage of the pre-densified composite core material eliminates the need for a relatively low viscosity melt to allow complete filling. This reduced shrinkage allows internal anode design modifications to be possible. One such internal design modification is to add a current carrying rod down the center of the core composite running the length of the anode. The motivation for having an imbedded conducting rod is to reduce the electrical path length through the high porous and thus reduced conductivity core composite. In an anode with a highly conducting rod imbedded in the core, the electrical path length is reduced from several inches to approximately 3/8 inch. Copper, titanium, and mild steel rods were investigated for this use. The resistivity testing of two anodes with a copper rod imbedded in the core composite showed a dramatic, ~10 times, reduction in the high temperature resistivity of the anode. However, when one of these anode was sectioned for post-mortem analysis, it was revealed that the copper rod had been completely absorbed into the composite core material during the filling process leaving behind a hole where the rod was initially positioned. The titanium rod showed a similar decrease in anode high temperature resistivity. The titanium rod remained intact after the filling process. Using the mild steel rod produced the most promising results by yielding a high temperature resistivity which is lower than the tested graphite

33

anode high temperature resistivity. The combination of the core composite attributes of reduced shrinkage, modulus, and strength is the key to allowing these types of anode design modifications.

Electrical Testing

In order to perform a pre-evaluation of the electrical performance of the developmental anodes and also as a quality control check on the filled anode integrity, a high temperature resistivity measuring device was designed and constructed. A high temperature device is needed due to the varied temperature dependence of electrical resistivity for different materials. With respect to the anode, the resistivity of the metallic core would be expected to decrease with temperature while the resistivity of the ceramic shell would increase. Thus, a high temperature measuring device was needed to gain accurate resistivity data. A schematic of the high temperature testing apparatus is shown in Figure 18. The high temperature resistivity measuring device uses a four point resistivity measurement scheme. The temperature control and data collection is performed by a Camile™ control system. The testing is performed in a controlled atmosphere furnace.

To graphically demonstrate the usefulness of this type of measurement device, Figure 19 presents a resistivity versus temperature graph for a ceramic anode and a graphite anode. This graph shows the dramatic decrease in the resistivity as a function of temperature for the ceramic anode as compared to the graphite anode which is relatively constant. The graph also shows that the electrical resistivity of the ceramic anode is very comparable to graphite at 700°C. At 700°C, the ceramic anode had a minimum resistivity of 0.645 mΩ-cm which is lower than the graphite's resistivity of 0.907 mΩ-cm. This anode design is shown in figure 20.
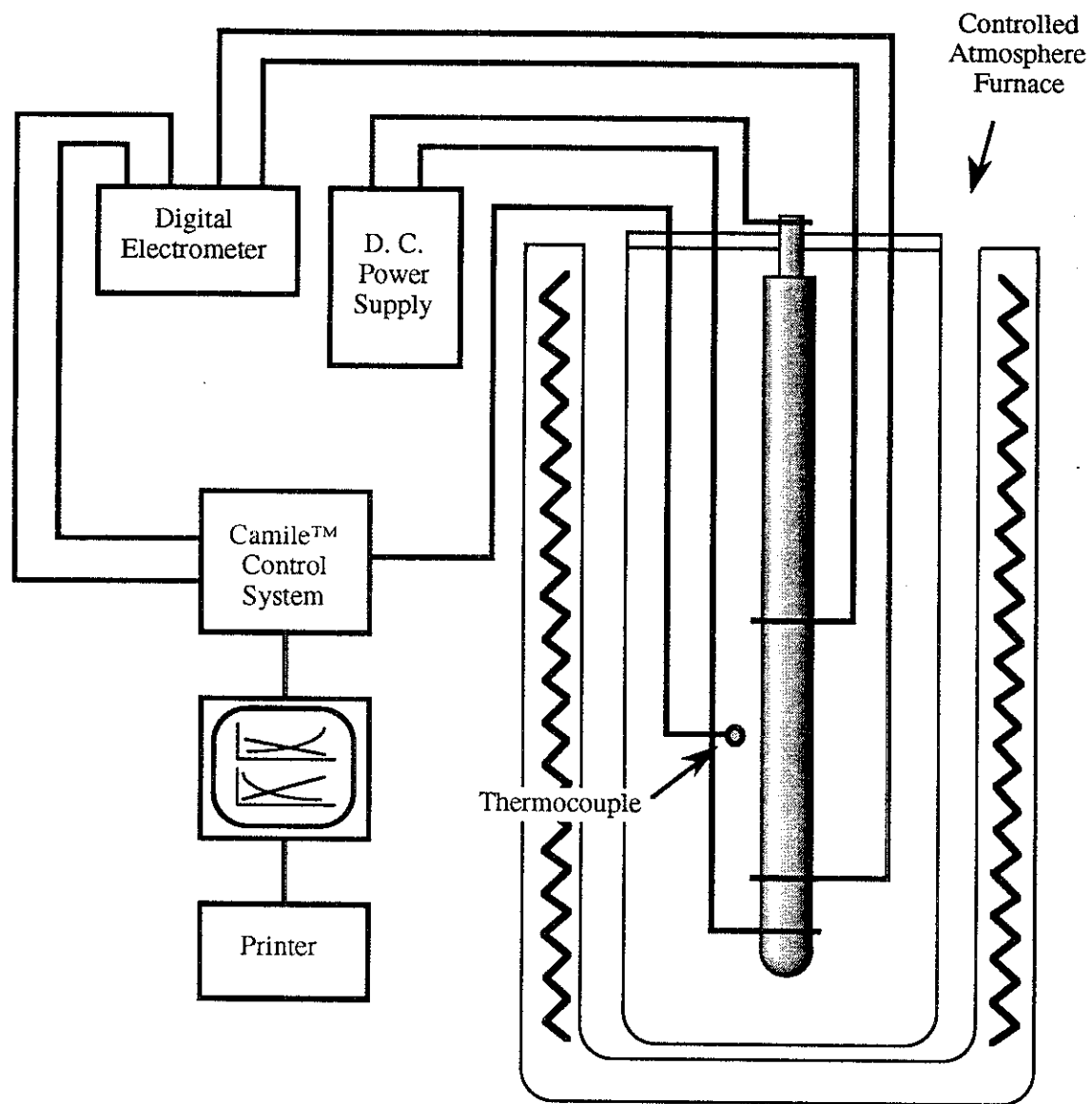
Figure 18, Sketch of the high temperature resistivity testing apparatus.
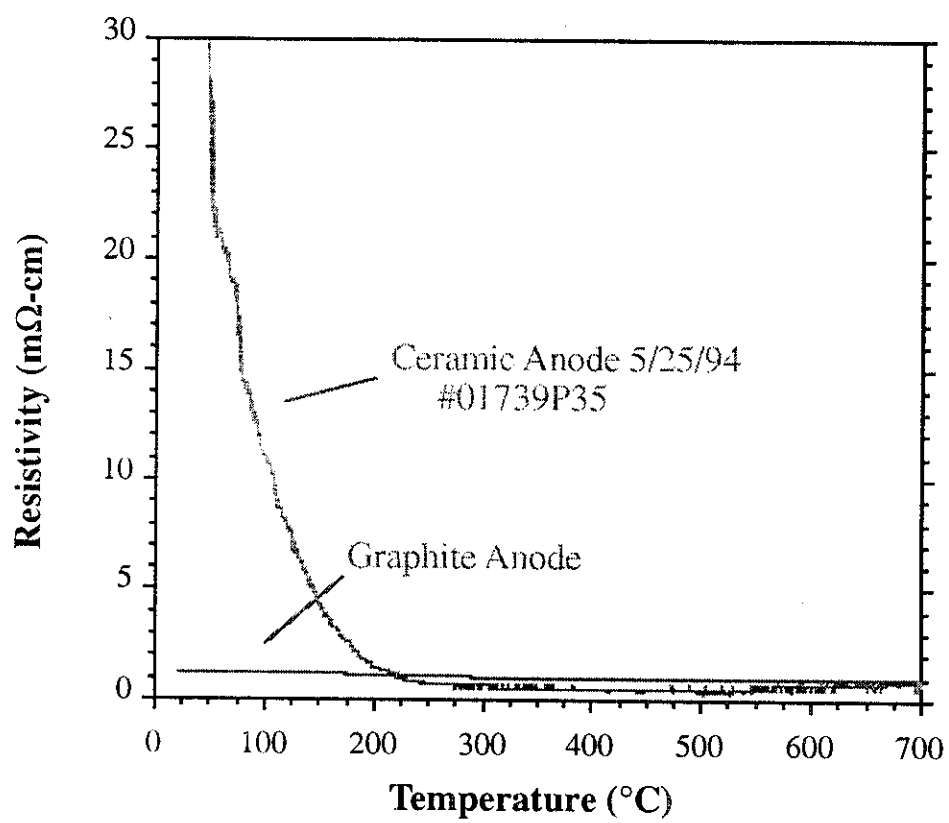
Figure 19, Resistivity versus temperature graph.

Gray iron push rod
(1/2" dia. x ~4" long)

Pre-densified SHS core material
60/40 wt. % Ti/Cu alloy with 60 vol. % TiC

Mild steel conducting rod
(1/4" dia. x 9" long)

Alloy coated shell interior
(75/25 wt.% Ti/Cu alloy)

Porous interlayer on shell interior

Ceramic shell
(TiO_2 with 5 mole% Ta_2O_5)

Figure 20, Sketch of lab scale ceramic anode with imbedded conducting rod.

Raw Material Cost Reduction

To ensure the eventual implementation of the ceramic anode into the production magnesium electrolysis cell, a preliminary cost analysis was completed. The analysis revealed that the cost of the raw materials was of potential concern. Reducing the expected ra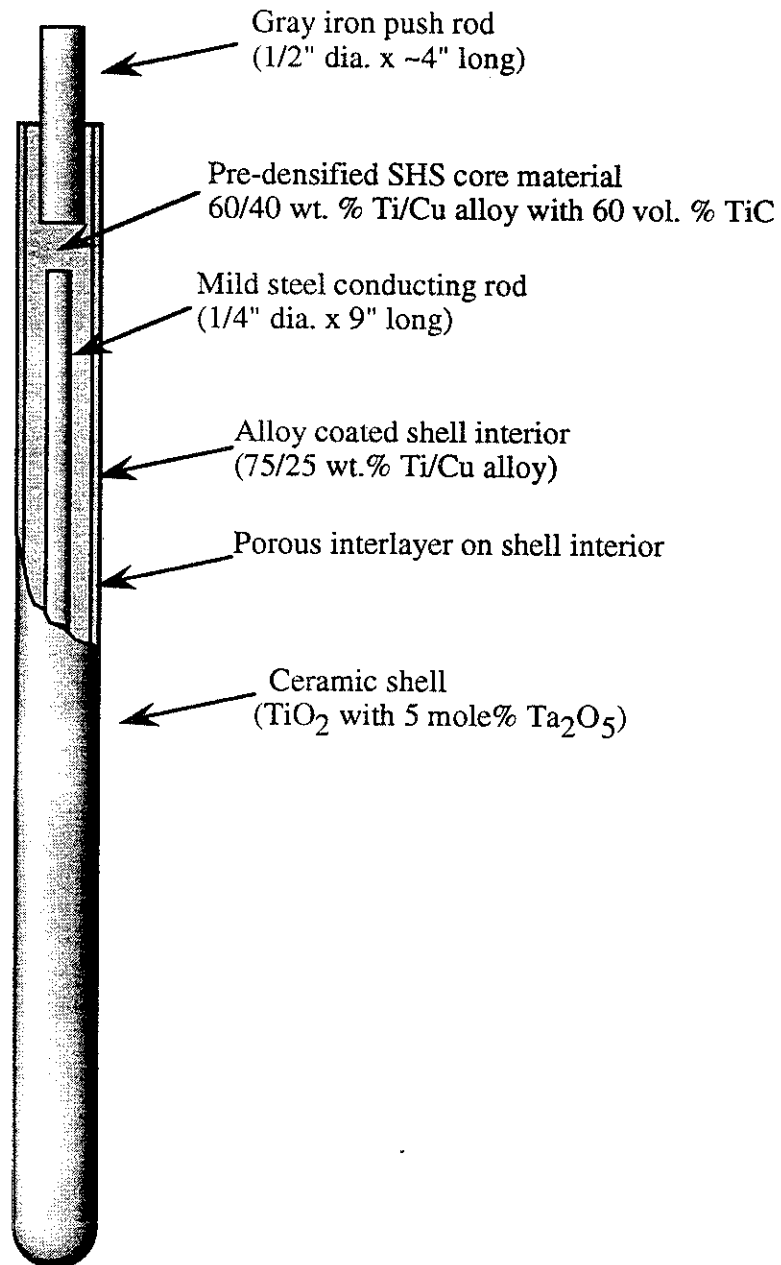w material cost while maintaining the electrical performance of the anode became a important development issue. The following work topics were directed at exploring different methods to reduce the cost of the raw materials to be used in the full scale anode:

1. Examine variations in the composition of the ceramic shell.
2. Investigate substitutions of less costly materials.
3. Introduce and demonstrate design changes to reduce overall material costs.

Ceramic Shell Composition Variations

The protective ceramic anode shell is a titanium dioxide ceramic doped with small additions of tantalum pentoxide. During the sintering process, this ceramic combination will form a solid solution material. When cooled, the resultant ceramic has high corrosion resistance as well as the unique property of being a semi-conductor (in general, ceramics are electrical insulators). While this ceramic shell is the enabling technology for this project, it also has the main raw material cost. More specifically, approximately 85% of the raw material cost comes from the 5 mole % tantalum pentoxide doping of the titanium dioxide ceramic. Thus, reducing the dopant level in the ceramic shell would lead to significant raw material cost reductions.

The titanium dioxide - tantalum pentoxide ceramic material will form a solid solution composite in the doping range of 1 to 5 mole % of tantalum pentoxide. A study was undertaken to evaluate the potential of reducing this doping amount while maintaining the electrical properties cause by the dopant additions. Dopant levels of 5, 3, 2, and 1 mole % were investigated. We were able to sinter all of these compositions into dense ceramic rods. The high temperature electrical properties of these rods were then tested. Figure 21 presents the results of this test series. This graph shows that there is no measurable change in the electrical properties of the ceramic composite when the dopant level is reduced from 5 mole % to 3 and then 2 mole % tantalum pentoxide. However, the electrical resistance of the 1 mole % dopant composite has a higher resistance and thus poorer electrical properties.

Anode shells of the 3 mole % tantalum pentoxide doping level ceramic were fabricated and were tested in the laboratory scale magnesium cell to investigate wear characteristics as compared to the higher level doped ceramic.

Material Substitutions

Material substitution was another raw material cost reduction route being investigated. Niobium pentoxide has been selected as a potential candidate to replace tantalum pentoxide as the ceramic shell dopant. Niobium pentoxide has similar electrical valence properties to tantalum pentoxide. Figure 21 shows a electrical resistivity data point that shows that a niobium doped titania ceramic has equivalent, if not slightly better, electrical properties compared to the tantalum doped system. The raw material cost for the shell could be reduced because niobium pentoxide is $1/4$ of the cost per pound than tantalum pentoxide and less weight (~44%) would be needed to reach the 3 % molar doping level due to its lighter molecular weight.

Anode Design Variations

There are several anode design variations that can be implemented to further reduce the raw material cost of the anode. A promising idea is to make a gradient ceramic shell that would have a "standard" titanium oxide - tantalum pentoxide lower portion and a pure titanium dioxide upper portion. Since only the lower portion of the anode shell will be electrically active, only the lower region of the shell needs to have the tantalum pentoxide dopant. Since the tantalum pentoxide is the dominant factor in the raw material cost, this gradient shell design would result in significant cost reductions.

We have explored two methods to make this gradient composition shell design. One method is to cast the ceramic shell in two halves. The lower closed end portion of the anode shell would be comprised of the "standard" titanium oxide - tantalum pentoxide composite. The upper portion would be cast as an open ended tube of pure titanium dioxide. The two halves would then be joined and sintered into a dense ceramic whole. Initial joining studies have shown that this approach is possible but would require further effort to increase the quality of the joint. The second method to achieve the gradient composition shell would be to cast the two halves as one piece by layering the slip as it is poured into the shell mold. Initial attempts at casting a gradient composition, small shell were successful.

Both of these cost saving measures require significant development work. The work to date has been performed in a exploratory proof of concept framework that can be more fully investigated if the raw material cost issues remains critical.
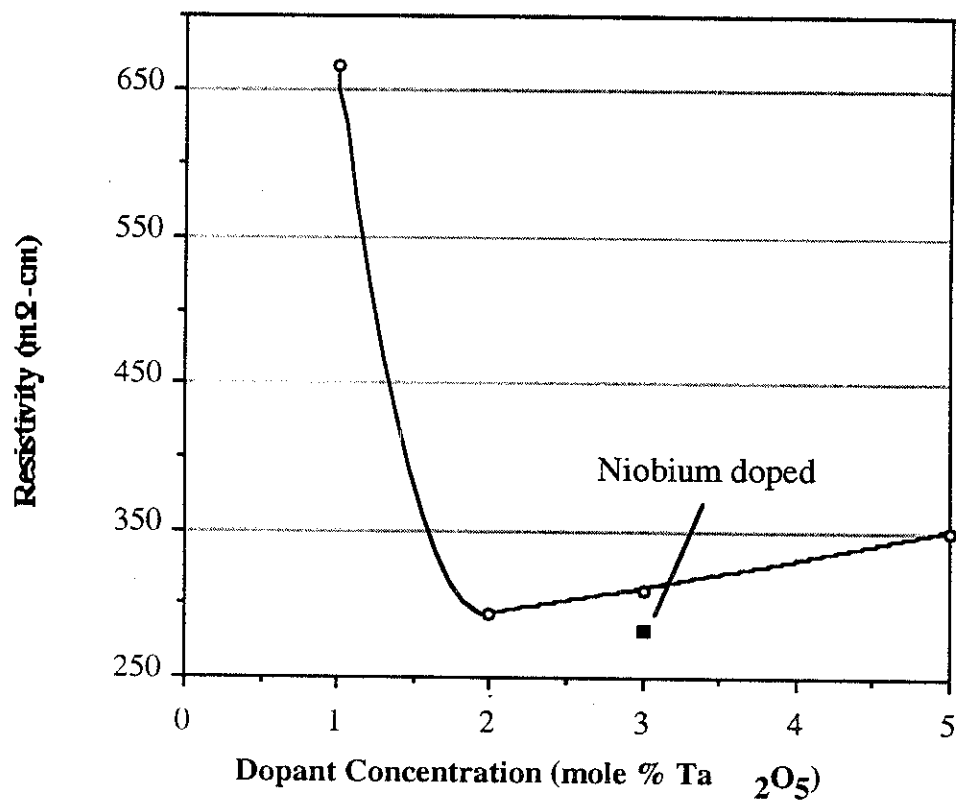

Figure 21, Graph of the electrical resistivity as a function of the tantalum pentoxide (Ta2O5) doping level of the titanium dioxide ceramic anode shell material.

Laboratory Scale Magnesium Cell Testing

Dimensional stability or corrosion resistance and good electrical performance of the ceramic anode are the key material properties. The corrosion resistance is tested in a laboratory scale, magnesium producing electrolytic cell. Figure 22 presents a sketch of this lab scale cell. A cell consists of a 2 liter quartz crucible which is supported on refractory brick in a furnace heated with metallic heating elements. The electrolyte is a molten mixture of chloride salts maintained at a temperature of 700-720° C. The cathode is a rectangular steel piece connected to the electrical supply by a steel rod. The rod is protected by an alumina sleeve, and clamped in position. The anode is also clamped in position in order to maintain the desired anode-cathode spacing, usually about 1 inch. Hydrous magnesium chloride is fed into the top of the cell to maintain the desired level of magnesium chloride in the electrolyte. The anodically produced chlorine was swept from the cell via a vacuum system. The molten magnesium was removed from the cell daily, and weighed to determine the cell efficiency. The cell was continuously monitored for current, voltage, and temperature. The cell operates using the same salt feed composition and operating temperature ranges used in the production magnesium cell.

Early attempts to fill the ceramic shell with a solid, thermal expansion matched metallic core composite met with limited success. During the filling process, the molten viscosity of the metallic composite core was too large to achieve the complete filling of the ceramic shell. This molten viscosity problem was overcome by using a pre-densified porous composite core material. Granules of the pre-densified porous material were used in the filling operation in place of a iso-pressed powder mixture used in the solid core designs. The nature of the pre-densified material does not require the low viscosity melt needed by the powder compact method to completely and uniformly fill the ceramic shell. This pre-densified porous material also has several additional advantages in anode design flexibility, weight, and cost.

Initial Magnesium Cell Lifetime Results

Two lab scale ceramic anodes were tested in the lab scale magnesium cell. Both of the ceramic anodes tested had similar design components as sketched in Figure 20. Both anodes designs had a Ta_2O_5 doped TiO_2 ceramic shell, alloy coating on shell interior, pre-densified porous core
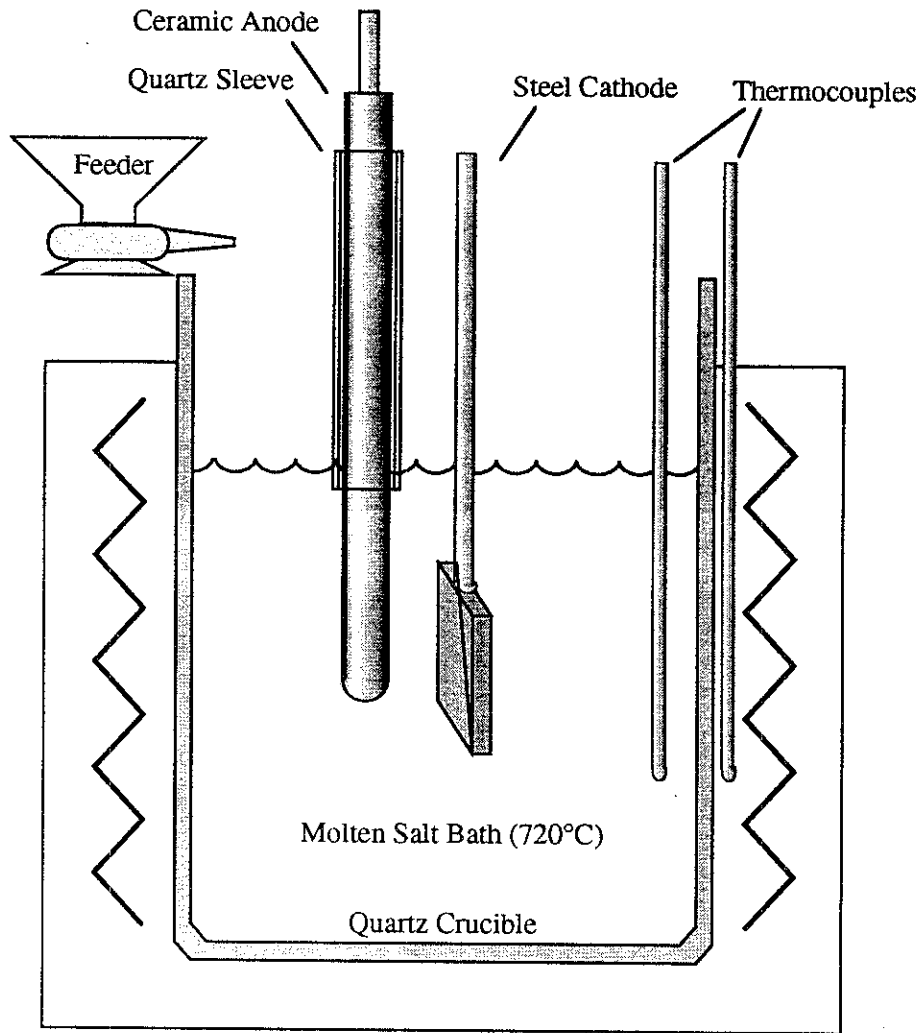
Figure 22, Sketch of the laboratory scale electrolytic cell.

with small additions of free alloy, an electrical connection rod, and an interior conducting rod. Both the alloy coating on the shell interior and the free alloy in the pre-densified core material serve to improve the bonding characteristics of the anode core and thus increase the electrical performance of the anode.

Magnesium cell testing of these two anodes met a premature end (One anode lasted 9 days while the second anode lasted only 3 days) when both anodes failed due to the formation of a small hole in the ceramic shell. These anode lifetimes are significantly less than the goal of 30 days.

42

Anode Failure Mode And Proposed Mechanism

The observed anode failure mode is the formation of a small hole in the protective ceramic shell. It is thought that once a hole forms and molten salts enter the anode interior, the operating voltage increases dramatically and the anode interior core is rapidly corroded/dissolved, effectively destroying the anode.

There are three basic potential causes for the onset of failure of the anode during testing;

- Chemical attack
- Physical flaws or cracks in the ceramic
- Electrical attack in the form of ohmic heating.

One theory explaining the formation of the small hole failure mechanism from electrical attack in the form of ohmic heating is depicted in Figure 23. This theory proposes that the point contact between the core granules and the ceramic shell would result in localized areas of relatively high current density. The localized ohmic heating or "hot spots" could in turn result in accelerated wear. Previous work has shown that the corrosion properties of the ceramic shell degrade at temperatures above 800°C. These "hot spots" are isolated areas of elevated temperature and thus high wear that would result in the formation of the small hole failure.

To address the potential ohmic heating of the anode shell, design modifications were made to the shell. Along with enhancing the physical bond between the core to the ceramic shell, the alloy coating on the shell interior has the added purpose of distributing the current from the granular core to the anode shell. In one tested design modification, the thickness of this alloy coating was increased from ~0.2 mm to ~0.5 mm. This anode was tested in the lab scale magnesium cell. This anode lasted only 5 days and failed by the same small hole failure mode.
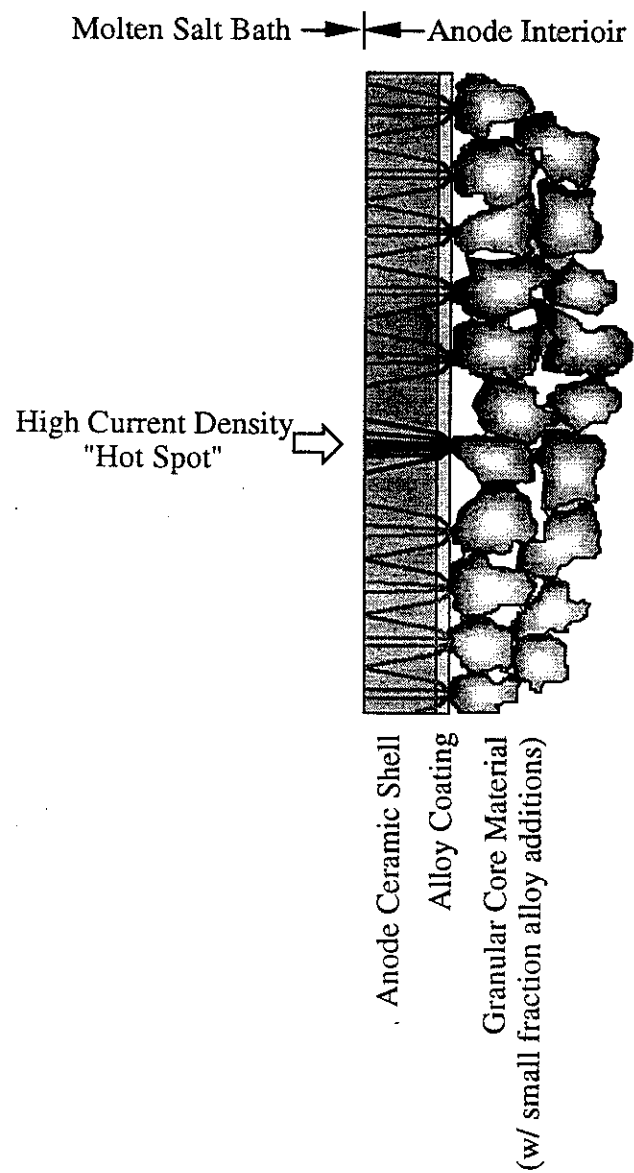
Molten Salt Bath →|←— Anode Interioir

High Current Density⇨
"Hot Spot"

Anode Ceramic Shell

Alloy Coating

Granular Core Material
(w/ small fraction alloy additions)

Figure 23, Proposed anode failure mechanism

4 4

Affect Of Furnace Atmosphere On Dopant Solubility

Accelerated chemical attack of the ceramic can also cause premature failure of the anode during testing. To investigate the likelihood that an accelerated chemical attack is causing the anode failure, the chemistry of the ceramic was investigated in depth. When heated to the sintering temperature of ~1300°C, the Nb_2O_5 doped TiO_2 ceramic material forms a solid solution which has the unique property of being electrically conducting. This solid solution has the rutile crystal structure of pure TiO_2 but with oxygen deficiencies which result in its electrical properties. When this shell material is subjected to a heat treatment step corresponding to the filling process step, the Nb_2O_5 dopant can precipitate out of the solid solution and migrate to the grain boundaries. During magnesium cell testing, these dopant enriched grain boundaries have been shown to be attacked by the corrosive magnesium cell atmosphere resulting in anode failure.

Current theory of diffusion and electrical conductivity in oxygen deficient binary oxides predicts that in an oxygen deficient solid solution like ours, the diffusion rate of the dopant can be significantly affected by the furnace atmosphere.[6] Subjecting the ceramic to a oxygen deficient or reducing furnace atmosphere may cause the dopant to precipitate out of the solid solution. This precipitation has been seen in our ceramic anode shells and the reduced corrosion properties of our anodes have been attributed to this occurrence.

Previous attempts at controlling this precipitation have centered around switching the dopant species from Ta_2O_5 to Nb_2O_5 and then reducing the dopant concentration from 5 mole % to 3 mole %.[7] With our new understanding of the possible affect of furnace atmosphere on the dopant solubility, the viability of performing all of the anode fabrication heat treatment processes in an air atmosphere was evaluated. The fabrication of the anode has three heat treatment steps. The first step is the sintering of the ceramic shell in a forced air furnace. The second step is an alloy coating process where a titanium-copper alloy is bonded to the shell interior. The final step is to melt a conducting titanium based cermet core inside the ceramic shell. Due to the reactive nature of titanium alloys, the coating and filling steps had previously been performed in an inert gas atmosphere or under vacuum. We found that with modifications to our coating and filling procedures and minor material changes, anodes with good electrical and physical properties could be fabricated with only slight modifications to existing equipment.

Figures 24 and 25 show a comparison of SEM micrographs of the ceramic shells taken from anodes that have been fabricated in a reducing atmosphere and one that was

Figure 23, SEM micrograph of the ceramic shell fabricated in a reducing atmosphere.
(Top of micrograph is the outside edge of the ceramic shell)

Figure 25, SEM micrograph of the ceramic shell fabricated entirely in an air atmosphere.
(Top of micrograph is the outside edge of the ceramic shell)

46

made in an entirely air atmosphere. The anode fabricated in the reducing atmosphere shows grain boundary enrichment of the Nb_2O_5 dopant (shown as the lighter phase in the micrograph) and void formation at the grain boundaries. This is compared to the micrograph of the anode fabricated entirely in an air atmosphere that shows no void formation or light phase at the grain boundaries that would correspond with grain boundary enrichment. This achievement marks further refinement of the final ceramic composition that should increase the corrosion resistance of the ceramic anode to the aggressive magnesium cell environment.

Ceramic Quality Impact on Corrosion Failure

It has been observed that the preferential etching of the ceramic dopant at the grain boundaries was the primary bulk material corrosion mechanism. Several processing changes were made to minimize and delay the onset of this form of corrosion (i.e. anode fabrication atmosphere modification). This achievement should increase the anode's bulk corrosion resistance properties. Unfortunately, through magnesium cell testing, the bulk material corrosion of the anode was unexpectedly found not to be the lifetime limiting wear property. Inspection of failed anodes revealed that isolated, pitting type corrosion may be causing the premature anode failure. It also appeared that these isolated severe corrosion areas may be related to the presence of small imperfections in the ceramic shell.

With great confidence, an anode fabricated entirely in an air atmosphere was tested in the laboratory scale magnesium cell. Despite having excellent electrical properties, the anode failed prematurely after only 9 days in the magnesium cell. Fortunately, this test was stopped shortly after failure preserving much of the pre-failure corrosion evidence. In the past, all anodes had failed during non-work hours and thus much of the evidence pertaining to the onset of failure was obscured by extensive post failure corrosion. In this test, the anode was rescued before significant post failure corrosion had occurred.

For this anode test, the test was halted due to the observation of a gradual rise in the cell operating voltage. In lab scale, magnesium cell tests, the cell load is held at a constant 10 amps (except for weekends when the amperage is dropped to 1 amp) resulting in an anodic current density of approximately 2 amps per square inch. The voltage is allowed to change or float to maintain the controlled amperage. It was found that during the final 16 hours of operation the voltage began to increase from a constant 3.5 volts to 7.5 volts at which time the test was terminated. When the anode was removed from the cell, there were several areas where evidence of the failure mechanism were still intact.

47

Because of the evidence of pre-failure corrosion structures, the anode was subjected to intense analytical tests. The anode was analyzed by secondary electron imaging (SEI), backscattered electron imaging (BEI), energy dispersive x-ray spectroscopy (EDS), and wavelength dispersive x-ray spectroscopy (WDS) elemental maps. Figure 26 presents a series of SEI micrographs showing a crack in the anode shell. Along this crack are irregularly spaced corrosion areas. These corrosions areas appear to be isolated high corrosion rate regions similar to pitting corrosion in metals.

Figure 27 shows a cross-section of another pitting type corrosion area but this time on the interior of the anode shell. This pit appears to coincide with a pre-existing surface crack. This surface flaw is most likely an artifact from the ceramic forming process. Similar greenware flaws of this type have been seen in other ceramic shells.[8] This interior corrosion indicates that the molten salts of the magnesium cell were present inside the anode with enough time to erode or pit the interior surface. It is our hypothesis that these molten salts gained entrance to the anode interior through small cracks in the protective ceramic shell. These cracks would have to be formed during testing in order to pass the pre-test inspection and small enough to escape the periodic anode inspection during operation.
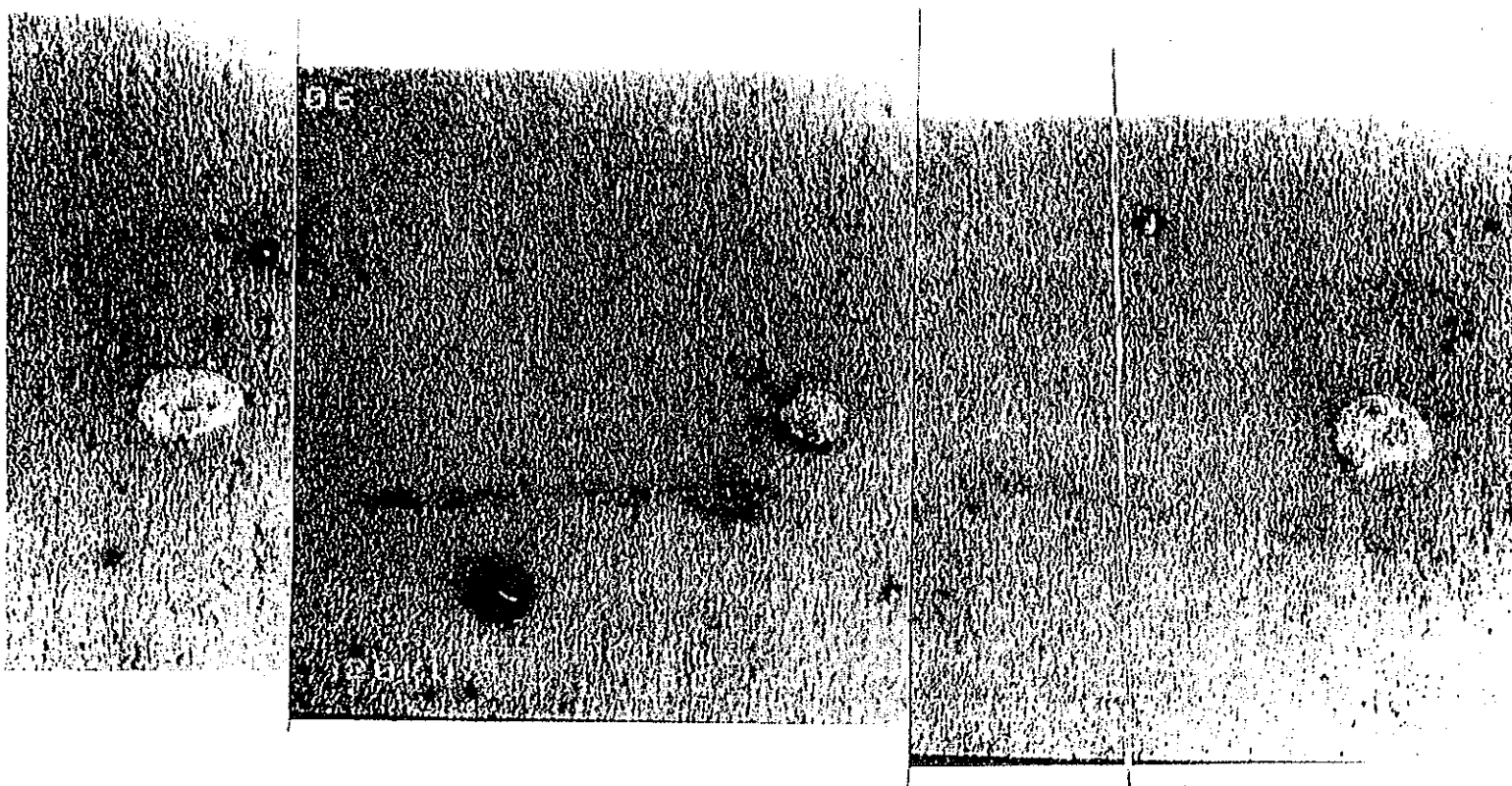
Figure 26. Series of SEI micrographs showing irregularly spaced corrosion areas along a crack in the anode shell.
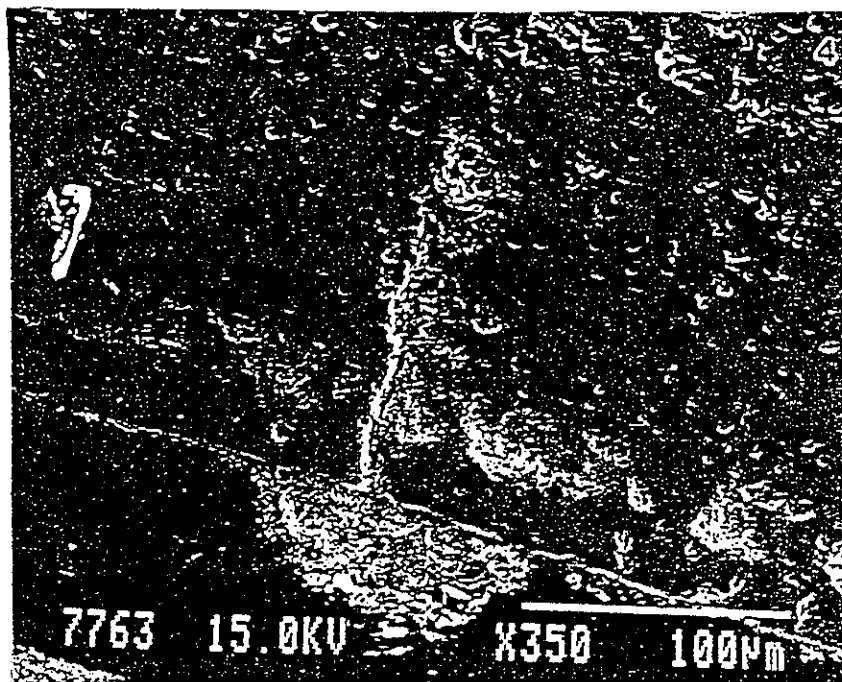
Figure 27. Cross-section of pitting type corrosion area.

Short Duration Anode Testing

To gather additional information about the onset of failure, two short duration magnesium cell tests were conducted. The first test was a four day operational test. The anode inspection after this short test revealed that the molten salts of the magnesium cell bath had reached the anode interior. The voltage history for this test showed no indication of when the salts might have entered the anode. It is thought that the presence of a conductive liquid inside the porous core of the anode would at least initially increase the electrical performance of the anode reducing the operating voltage for a short period before interior corrosion becomes severe. Also, no clear evidence of a crack in the ceramic shell was evident.

A two day test was conducted in an attempt to catch clear evidence of the onset of anode failure before the molten salts reach the anode interior. Once again, there were no fluctuations in the operating voltage during the two day test. However, post-mortem analysis showed that this anode also had molten salts inside the anode. During cooling of the anode, a ~2 inch, rust colored line appeared along one side of the anode running along the long axis of the anode. Further inspection revealed that this line was in fact a hair-line
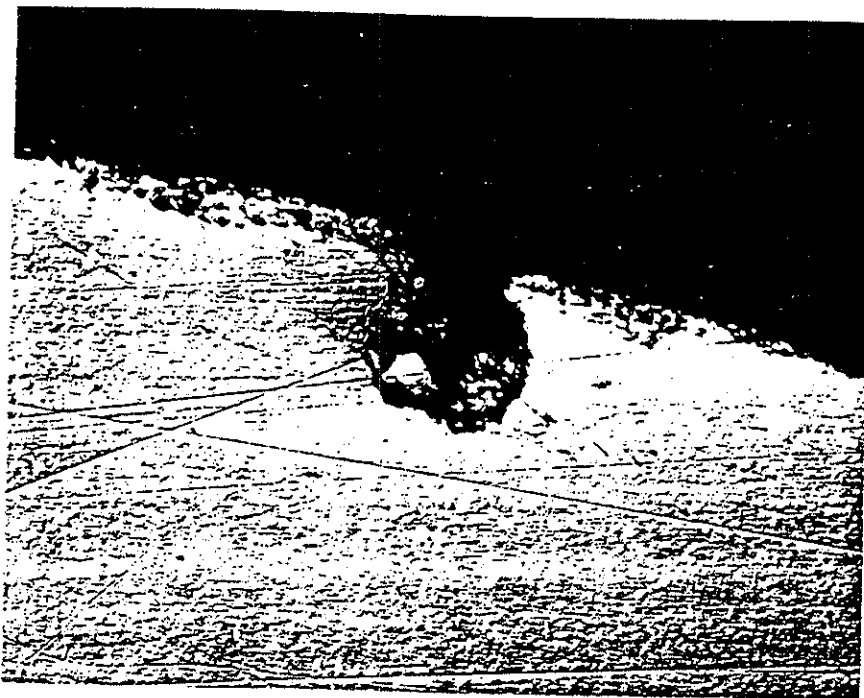
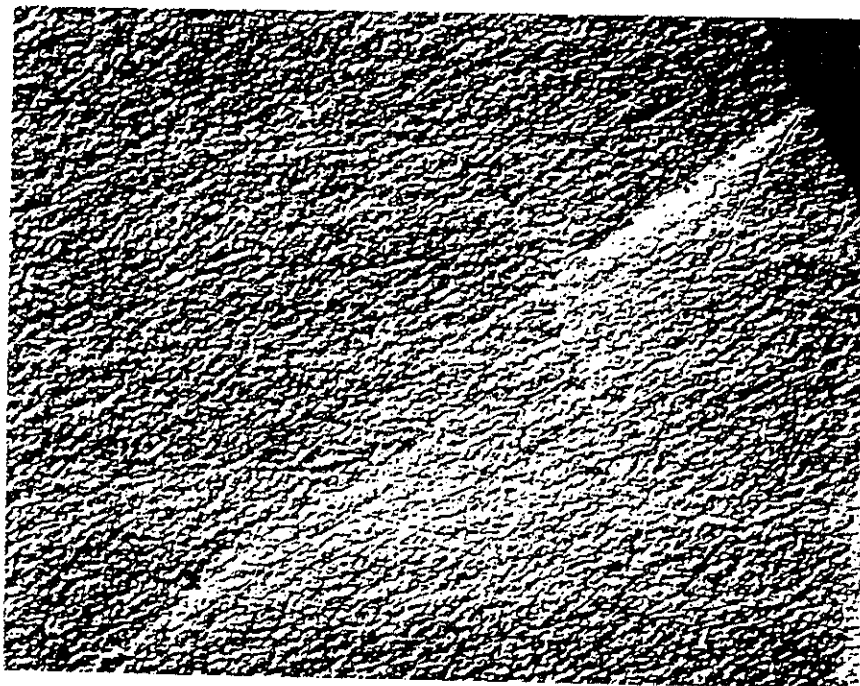Figure 28. Optical micrograph of the pinhole defect.

Figure 29. Optical micrograph of a heeled crack that occurred in the green state

Anode Lifetime Testing

With improved fabricating procedures and an increased understanding of the anode corrosion mechanisms, there was renewed confidence in achieving the 30 day lifetime magnesium cell tests. With these recent technical strides, the direction of the research team has focused more tightly on reaching the project's testing milestones. During all steps of the fabrication process, these anodes are subjected to numerous quality control nondestructive evaluation (NDE) such as: fluorescent dye penetrant tests, optical microscopy, and room temperature resistivity measurements.

After arriving at the Dow's Inorganic Research Laboratory in Freeport, Texas, the first of these improved anodes were tested at an operating current of 6 amps. This anode achieved the milestone of surviving 30 days of continuous operation in the lab scale magnesium cell. The anode was removed from the test cell after 32 days while still intact.

A second anode of similar design was tested at the same operating conditions. This anode also reached the 30 day lifetime goal. The anode was removed from the cell after 34 days of testing. This anode was also intact and had the appearance of being able to survive for significantly longer. Both of these tests were terminated so that confirmation tests could be run and the 6 anode, 30 day test milestone could be meet within the tight program schedule. Both of these anode test fully meet the requirements outlined in the testing plan and thus are valid, successful tests.

Wear Measurements And Procedures

As the anode lifetime gets longer, it becomes possible and important to measure the anode wear rate to determine the expected production anode lifetime. We have found that determining the wear rate of the anode is not a trivial matter. Simple displacement measurements are not accurate due to the formation of hard deposits on the ceramic surface during cool down. In removing these deposits, some of the ceramic shell is also removed or chipped away making the displacement measurements inaccurate. Direct diameter measurements of the anode before and after testing have also proven unreliable. The ceramic anodes tend to be slightly out of round making the measurement of the very small wear numbers difficult even when attempting to measure at the exact location on the anode before and after cell testing.

A microscopic technique has been developed that has shown to produce repeatable and reasonable wear numbers. The technique utilizes a low magnification optical

microscope with an attached digital camera. The anode is first mounted on a X-Y micro-manipulator platform. A straight edge is then mounted on the platform in close proximity and parallel to the anode. A series of digital images are then taken and printed on a 8" by 5" paper. Enough pictures are taken to cover an approximately 1.5 inch area that traverses the working and non-working portion on the anode. The pictures can then be re-assembled using the photographed straight edge as a guide. A large straight edge can then be used to reveal the amount of wear by comparing the deviation of the working area surface from the interpolated reference line taken from the non-working surface. Wear rates for both 30 day, 6 amp magnesium cell test anodes have been measured. These wear numbers are shown in table IV.

Table IV. Anode wear in laboratory scale magnesium cell testing

Anode ID Number	Operating Amperage	Test Duration	Wear (mm/yr)	Wear (μm/Amp-hr)
9301739P97	6 Amps	32 days	2.1 mm/yr	0.073 μm/Amp-hr
9301739P100	6 Amps	34 days	1.5 mm/yr	0.071 μm/Amp-hr

These are the first reliable wear numbers obtained on the niobium doped titanium dioxide ceramic anode. The measured wear for this niobium doped material compares favorably with the 3.3 mm/yr wear number reported for the tantalum doped ceramic anodes[1] that were being developed and tested in the first phase of this cooperative agreement. Recall that the raw material change from tantalum pentoxide to niobium pentoxide was prompted by a rough economic evaluation of the price to manufacture the full scale anode. It was found that the dopant switch would result in a ~60% reduction in the total raw material cost of the assembled anode. Electron probe and transmission electron microscopy revealed that the dopant material change also appeared to reduce the precipitation of the dopant to the grain boundaries. This dopant migration was identified as a major anode wear mechanism[2].

Preparing For Higher Current Density Tests

The laboratory scale magnesium cell testing plan included in the program proposal defines the cell operating range of 5 to 20 amps current load on the anode. After the two successful lifetime tests at a 6 amp operating amperage, the decision was made that higher amperage tests would be valuable in assessing the expected performance in the production cell that operate at higher current densities. However, due to the anode and cathode geometry differences, direct comparison between the lab scale test results and the expected production cell performance can not be made. This change in testing procedure was also motivated by the loss of Government funding for Phase III of the cooperative agreement. Without Government assistance, the Dow's magnesium business decided that the technical risk associated with scaling-up and implementing the ceramic anode into production would need to be minimized if the project was going to proceed without Government assistance. To minimize the technical risk, higher operating current tests would be necessary to determine the anode's sensitivity to operating current range or robustness.

To start evaluating the anode lifetime sensitivity to operating current density, an anode was tested at the higher operating current of 10 amps. This anode had a similar design to that of the two anodes that had successfully survived the 30 day test running at 6 amps. This anode failed after 24 days of operation. While this anode did not reach the 30 lifetime goal, 24 days of operation was still longer than previous tests on 'un-improved' anodes.

It was felt that ohmic heating and the cathode geometry may have impacted this test. This brings up the question of the effect of cell geometry on the effective current density that the anode experiences. Referring back to the lab scale magnesium cell's geometry pictured in figure 21, the cylindrical anode is located in a relatively large bath of molten salts along with the rectangular, flat steel plate cathode. Comparing this lab scale cell to the production cell, shown in figure 30, the difference in cathode design and relative molten salt bath volumes between the two cell geometries is evident.

The lab scale cathode design is a concern due to the possibility of preferential wear of the anode directly facing the cathode. In the lower current tests, the anode appears to be wearing evenly about the entire circumference of the anode.

Figure 30. Production cell geometry sketch

$$MgCl_2 \rightarrow Mg + Cl_2$$
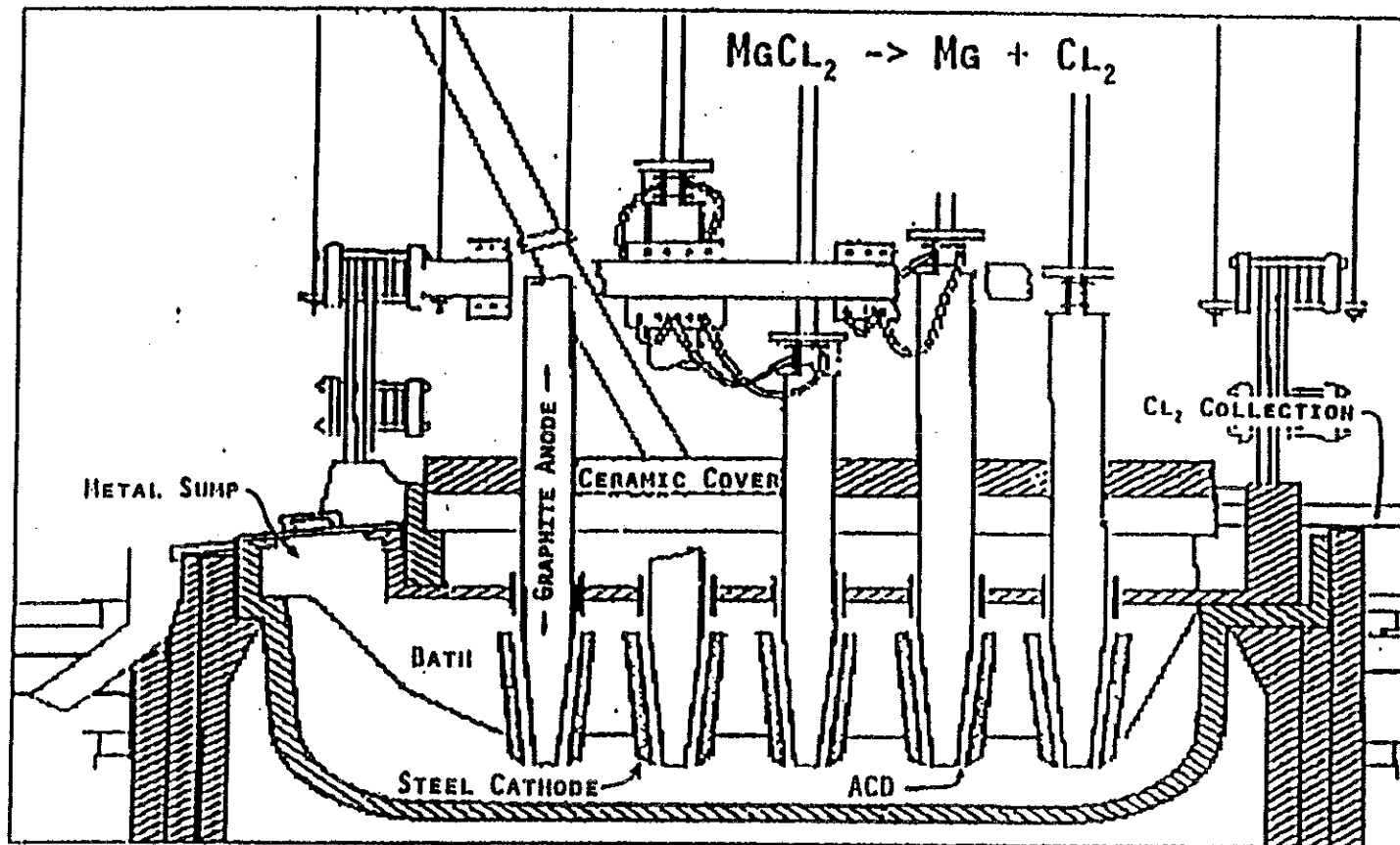
DOW MAGNESIUM CELL

Received from Jay Anderson, EG&G Idaho, Inc., July 12, 1993 (BDTN)

The even wear can be attributed to the highly conductive molten salt bath. However, at higher operating current, there may be a concentration of the current density on the anode facing the cathode causing increased wear in that region. After the completion of the higher current density tests, the anode was inspected for this type of wear pattern. If found to be the cause of the anode failure, the fact that this unsymmetrical wear is an artifact of the test cell geometry and will not be present in the full scale magnesium cell will have to be considered.

The second disparity between the lab scale cell and the production cell is the relative molten salt bath volumes compared to the anode surface area. This is a significant difference due to the function of ohmic heating in the production cell. At full capacity operation, the production cell is heated solely by the ohmic heating of the anodes and electrolyte. In this way, the temperature of the molten salt bath is maintained in a very uniform manner. In contrast, the lab scale cell is heated by surrounding heating elements due to the larger relative bath volume to the anode surface area. The bath temperature is controlled via a thermocouple in the bath. Unfortunately, this control scheme does not directly reflect the temperature at the anode surface where additional heat is being added to the system through ohmic heating. This is a concern because modest (~80°C) increases to the molten salt bath result in accelerated corrosion of the ceramic anodes[1]. Anode to be tested at 20 amps were modified to incorporate an imbedded thermocouple to evaluate the magnitude of this temperature differential that may arise from ohmic heating.

High Current Density Tests

Two extremely high quality anodes were fabricated, subjected to extensive non-destructive analysis, and then sent to Texas for laboratory scale magnesium testing at the high operating current of 20 amps. These anodes had a similar design to that of the two anodes that had successfully survived the 30 day test running at 6 amps but also included the imbedded thermocouple to detect any ohmic heating. During the testing, the temperature recorded by the imbedded thermocouple was consistently ~10 °C lower than the surrounding molten salt bath. This indicates that any ohmic heating that was occurring was being overwhelmed by the cooling from the exposed top section of the anode that protrudes out of the magnesium cell into the cooler atmosphere of the surrounding laboratory fume hood. Simply put, the anode is acting like a large cooling fin. Thus, the proposed failure mechanism of gross ohmic heating has been disproved. This first anode tested at 20 amps operating current failed after only 6 days of operation. The second anode was then tested at the same operating conditions. This anode also showed the cooler

57

temperature at the anode interior compare to the cell bath temperature. This second anode tested at 20 amps operating current failed after only 3 days of operation. Both of these anodes failed by the formation of pitting type corrosion.

The above results reflect a strong dependence between corrosion resistance and operating current. Post mortem analysis revealed that neither of the anodes showed significant asymmetric wear on the face nearest the cathode. This indicates that the geometry effect of the laboratory scale magnesium cell does not have as large and effect on wear as previously thought. The theory of gross ohmic heating was also discounted by the thermal couple data. However, the thermal couple data does not rule out the presence of isolated, small temperature rises caused by various sources could result in the accelerated wear seen. Microscopic imperfections in the shell could be exploited by the very mobile molten salts producing a highly conductive route for energy flow, acting almost like a lightning rod across the ceramic. Much attention throughout the program has been directed at minimizing these types of microscopic flaws. Unfortunately, higher current densities appear to exploit even the smallest of flaw populations. This raises some hard questions about the ceramic anode robustness with respect to both sensitivity to operating conditions and to tolerance of even small flaw population in the ceramic shell. These issues present significant challenges to overcome before anode implementation.

Scale-up Partner Interactions

Identifying a partner to scale-up the anode technology was an important task during the second phase of the cooperative agreement. Once identified, the scale-up partner would need to be brought up to speed on the technology. Ipsen Ceramics was selected to fabricate a full scale ceramic anode for magnesium metal production as a subcontractor in phase III of the program base on their production and development capabilities. Figure 31 is a sketch of the proposed full scale anode. Ipsen was identified as a potential partner along with three other companies. Ipsen Ceramic's initial selection was made due to their advertised ceramic products of similar large dimension. Ipsen ceramics is a wholly owned company of Abar Ipsen Industries, (a several billion dollar sales company). Ipsen ceramics itself, is very small reporting 1993 sales of ~3.6MM.
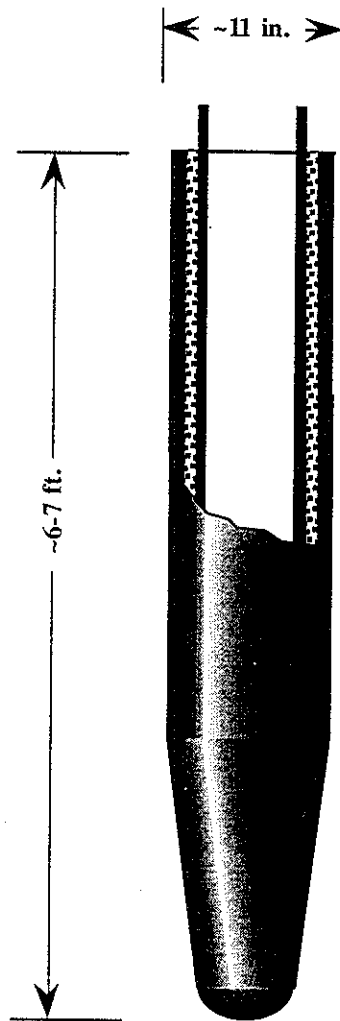
Figure 31. Full scale anode sketch

Some of the key capabilities we were looking for in a scale-up partner are the following:

- Ability to cast large, closed end tubes
- Ability to sinter large tubes
- Familiarity with casting fine particle size ceramics
- Developmental facilities
- Good engineering support
- Desire to work on project
- Flexibility to consider fabricating entire anode

Ipsen Ceramics was found to have the production capability along with all of the above capabilities except a slight weakness in developmental facilities

To addresses critical scale-up issues, a joint development project was initiated with Ipsen Ceramics. This joint program was designed to include a general evaluation of the quality of Ipsen's large ceramic parts along with a direct lab scale anode shell comparison. For the lab scale shell comparison, Ipsen made casting molds with the lab scale anode mandrel and then cast and sintered three shells with their similar product, 995 Alumina. These anodes where then delivered to Midland for flaw testing. The second stage was then to cast and sinter 2-3 shells with slip provided by Dow Chemical to provide a direct comparison to shells produced by Dow Chemical. The final task was to mill, cast, and sinter the Dow powder formulation with Ipsen's standard binder system. These anodes where also sent back to Dow for evaluation.

Along with this joint development program, Ipsen delivered a large slip cast closed end tube for Dow to evaluate for casting defect increases to expect during scale-up. Results from optical microscopy analysis reveal that Ipsen's large tube does have casting defects similar to which we had seen and deemed unacceptable in our own cast parts cast in the early stages of the program. Once the developmental anodes were received from Ipsen, they were subjected to dye penetrant testing and also sectioned, mounted and polished for micrographic analysis. During this analysis, we found that the shell produced by Ipsen had a significant amount of exterior surface bubbles or pinholes casting defects. However, there shells did not have any greenware drying defects.

A working meeting was arranged in which the entire casting and sintering processes was reviewed at Ipsen Ceramics. The outcome of this meeting was the successful transfer of technology associated with the handling of the anode shells. During this technology transfer several key processing steps were identified as direct causes of the defects that were seen in the ceramic shells. Fortunately, these exact processing problems had already been dealt with and solved in the development work performed in Midland.

Ipsen Ceramic will use these processing improvements in completing the third task in our joint development program. In the third task where Ipsen milled, cast, and sintered the Dow powder formulation with their standard binder system and processing equipment. These anodes shells incorporating the Dow technology showed marked improvement.

Summary

Significant steps have been made in development of a dimensionally stable ceramic anode to be used in magnesium metal production. A stable anode would allow optimization of the spacing between anode and cathode yielding significant energy savings of per pound of magnesium produced. In addition, the currently used graphite anodes are consumed during electrolysis at a cost of up to $3.3 MM/yr. There is also considerable projected labor savings from the elimination of the need to reposition the anodes to maintain the anode's electrical efficiency. Not having to adjust the anode would allow better sealing at the furnace/anode interface for substantial environmental benefits.

Strides have been made in the fabrication of the ceramic anode with the invention and development of a novel pre-densified composite core material which uses the SHS processing route. By using this pre-densified composite material with standard anode fabrication procedures, completely filled, crack free anodes can be produced. This SHS core material has the unique properties of providing a strong bond with the ceramic while having a good thermal expansion match with the shell ceramic. The ceramic shell processing techniques have also been addressed in painstaking detail. The early laboratory scale magnesium cell testing revealed that the quality of the ceramic shell used for the protective barrier against the corrosive cell environment was critical to the survival of the anode. Though the course of this project, state of the art slip casting techniques were used and advanced in the pursuit of a virtually flaw free ceramic anode shell. A program was initiated with our designated scale-up partner to transfer our slip casting technology developed in the program and also to identify the challenges that might be faced during scale-up.

The testing goal for Phase II of the cooperative agreement was to demonstrate six anodes surviving a 30 day test lifetime with acceptable wear rates and electrical performance in a laboratory scale magnesium cell test. During this program, two successive anodes were tested and exceeded the 30 day cell lifetime goal with excellent wear characteristics. Unfortunately, a notification that the Government portion for Phase III funding would not be available to assist in scale-up of the project shifted the testing emphasis to more aggressive laboratory tests to evaluate the technical risk associated with continuing the anode replacement project without Government funding. Anodes tested at the more aggressive, higher amperage testing conditions failed from the formation of pitting type corrosion similar to that seem in metal corrosion. The failure of the anode to survive the more aggressive cell tests revealed that the ceramic anode had a rather narrow operating region. This lack of robustness of the dimensionally stable ceramic anode resulted in the Dow Chemical Company's Magnesium Business to make the decision not to continue the project

without continued Government support.

62

References

1. a. A. L. Finley, S. F. Spangenberg, and D. J. Searson, "Low Wear Magnesium Cell Anodes," CRI 774569, Lab. Code NEI-447, June 10, 1977.

   b. J. H. Muhs, "Conductive Molten Metal Cores for Ceramic Magnesium Anodes," CRI 780721, Lab. Code NEI-462, December 30, 1977.

   c. A. L. Finley and D. V. Livingston, "Ceramic Magnesium Cell Anode," CRI 785929, Lab. Code NEI-488, August 10, 1978.

   d. A. L. Finley, D. J. Searson, and J. Amrozowicz, "Initial Lifetime Studies for Ceramic Magnesium Cell Anodes," CRI 811351, Lab. Code NEI-537, April 6, 1981.

   e. A. L. Finley, D. J. Searson, and J. Amrozowicz, "Data Review - Ceramic Anode Lifetime Study," CRI 811596, Lab. Code NEI- 542, May 5, 1981.

   f. A. L. Finley, D. J. Searson, and J. Amrozowicz, "Grain Size Reduction in Ceramic Magnesium Cell Anodes," CRI 814204, Lab. Code NEI-557, October 28, 1981.

   g. S. F. Spangenberg, A. L. Finley, and D. J. Searson, "Electrolytic Cell and Anode for Molten Salt Electrolysis," U.S. Pat. No. 4 370 216 (1983).

   h. S. F. Spangenberg, A. L. Finley, and D. J. Searson, "Process and Anode for Molten Salt Electrolysis," U.S. Pat. No. 4 448 654 (1984).

2. H. Hahn, J. Logas, and R. S. Averback, "Sintering Characteristics of Nanocrystalline TiO_2," *J. Mater. Res.*, 5 [3] 609-14 (1990).

3. H. Wohlfromm, P. Pena, J. S. Moya, and J. Requena, "Slip Casting of TiO_2," pp. 1.211-1.217, in Euro-Ceramics, Vol. 1, *Processing of Ceramics.* Edited by G. de With, R. A. Terpatra, and R. Melselaar. Elsevier Applied Science, New York, 1989.

4. L. I. Verba and E. V. Degtyareva, "Rheological and Technolgical Properties of Titanium Dioxide Slips and the Properties of the Castings," *Ogneupory,* **1978**, [3], 28-33.

5. S. A. Anderson, B. D. Bubaker, M. J. Semer, A. G. Haerle, R. D. Varjian, "Development of an Inert Ceramic Anode to Reduce Energy Consumption in Magnesium Production: Progress Report for 1/1/93 to 12/31/93," GOV-ATAR-94-218, Dec 10, 1994.

6. P. Kofstad, <u>Nonstoichiometry, Diffusion, and Electrical Conductivity in Binary Metal Oxides</u>, John Wiley & Sons, Inc, New York (1972).

7. S. A. Anderson, et al., "Development Of An Inert Ceramic Anode To Reduce Energy Consumption In Magnesium Production; 2nd Quarter Report" Cooperative Agreement DE-FC07-91 ID13133, July 31, 1995.

8. Dr. Richard Haber, Rutgers Center for Ceramic Research, Private communication, December, 1995.